LENGTH RESTRICTED MOLECULAR DYNAMICS (LRMD) SIMULATION OF NANOMETRIC CUTTING

By

NAGASUBRAMANIYAN
CHANDRASEKARAN

Bachelor of Engineering

University of Madras,

Madras, India

1995

Submitted to the Faculty of the
Graduate College of the
Oklahoma State University
in partial fulfillment of
the requirements for
the Degree of
MASTER OF SCIENCE
May, 1997

LENGTH RESTRICTED MOLECULAR
DYNAMICS (LRMD) SIMULATION
OF NANOMETRIC CUTTING

Thesis Approved:

R Noorani

Thesis Adviser

Lloyd M. Kaff

Don A. Lucca

Thomas C. Collins

Dean of the Graduate College

ACKNOWLEDGEMENTS

"Matha Pitha Guru Deivam"

This sanskrit sloka emphasises the order in which prayer has to be offered by a person. Matha (Mother), is the source of our existence in this world and so, gets the first priority, as without her one would not be in this world. Pitha (Father), is a person who guides and makes sure his child follows the right path. His responsibility is to direct his child to a proper Guru (Teacher). Guru is the person who opens our mind and leads us to the path of knowledge, and hence towards Deivam (God).

I wish to express my sincere thanks to my parent's for their confidence in me. I would like to thank them for their encouragement at times of difficulty, love and understanding. Special thanks are due to my sister for her inspiration, motivation, love and guidance.

I would like to express my sincere appreciation to my advisor, Dr. Ranga Komanduri for his intelligent supervision, constructive guidance, inspiration, motivation and friendship. My sincere appreciation extends to Dr. Raff for introducing me to the concept of Molecular Dynamics and for providing guidance and encouragement throughout the study. I would also like to thank Dr. Lucca for his invaluable guidance and encouragement in the field of ultra precision machining

I wish to express my sincere gratitude to Dr. Ali Noori Khajavi for his constructive guidance, assistance, encouragement and friendship. I wish to extend my gratitude to K. Mallika for assistance in taking photographs of the simulation process. I wish to extend my gratitude to R. Parthasarathy for helping me to work with simulink.

Special appreciation are due to Prof. Hou and Dr. Ran Pan for their suggestions and assistance in this study. Thanks are also due to Rajesh Iyer, Vinoo Thomas, Cetin Murat, Ming Jiong and other research members of our group for their support and helpful converstaions.

Finally, I would like to thank the Department of Mechanical and Aerospace Engineering for providing the opportunity to pursue M. S. at Oklahoma State University.

TABLE OF CONTENTS

LIST OF TABLES

LIST OF FIGURES

CHAPTER 1

INTRODUCTION

1.1. INTRODUCTION TO ULTRAPRECISION MACHINING

Nanometric cutting involves material removal at extremely small depths of cut on the order of a few nanometers. Material removal at this level occurs in such processes as Ultra Precision Machining (UPM), Ultra Precision Grinding (UPG), and polishing. In UPM, a single point cutting tool (generally single crystal diamond) is used to finish parts (workmaterials are generally non-ferrous materials such as aluminum, copper etc. or semiconducting material such as silicon, germanium etc.) on a rigid, high precision machine tool. This technology was pioneered by researchers at Lawerence Livermore National Laboratory (LLNL) lead by Bryan (1979). It is used in the manufacture of optical mirrors, lenses, computer hard discs etc. In UPG, a multipoint grinding wheel is used to finish both metals, ceramics, and glass components. McKeown (1987) of Cranfield Unit of Precision Engineering (CUPE) pioneered this field. Many machine tool builders,

including Moore machine tool and Rank-Pneumo in the USA and other manufacturers in U.K., Japan, and Europe have implemented this technology.

Taniguchi (1983) defines UPM as those processes or machines by which the highest possible dimensional accuracy can be achieved at a given point in time.

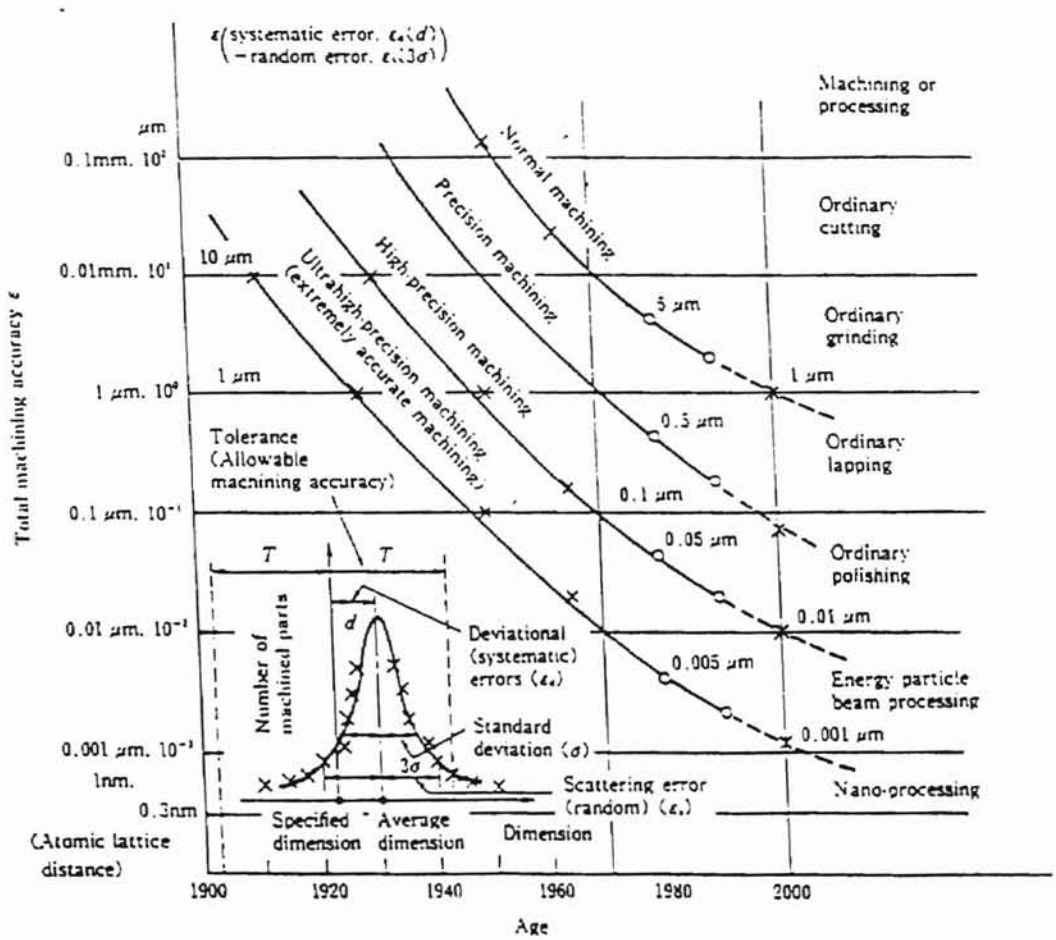

Fig. 1.1 Progress of machining accuracy achieved with respect to time during 20th century (after Taniguchi 1983)

Figure 1.1 referred to as the "Taniguchi Curve" shows the progress of machining accuracy with time. As the technology advances the geometric accuracy and surface finish requirements of parts increases. From Figure 1.1 it can be seen that what was considered to be highest achievable accuracy 10 years ago is considered as normal machining today. According to Taniguchi in the early years of the 21^{st} century the attainable processing accuracy will reach the nanometer level and it appears that today's UPM will be tomorrow's conventional machining. In general, UPM can be defined as a technique to produce high degree of surface finish (R_a of the order of a few nanometers) by removing material at extremely low removal rates (on the order of few angstroms). It is used in the manufacture of optical, mechanical, and electronic components, such as computer hard discs, lenses, mirrors for inertial confinement fusion reactor etc. It is carried out on an extremely rigid, high precision machine tool using a single crystal diamond tool when finishing non-ferrous materials such as aluminum, copper etc.

UPM/UPG are enabling technologies that have been used succesfully to extend the limits of geometric accuracy and surface finish of parts to nanometric level. Table 1.1 sets out in broad terms the manufacturing tolerances of components used in mechanical, electronic, and optical system products after Taniguchi (1983) by McKeown (1996). Most of the advanced technology products fall in the micro-technology regime (capability of one micrometer) and some in the nanotechnology regime (capability of 1 nm accuracy). This necessiates a continuous development of manufacturing technology, UPM tools, and associated equipment.

Table 1.1 Tolerance Band and Applications of Conventional Machining and UPM *

	Tolerance band	Mechanical	Electronic	Optical
Normal machining	200 μm	Normal domestic appliances and automotive fittings etc.	General purpose electrical parts, e.g. switches, motors and connectors	Camera, telescope and binocular bodies
	50 μm	General purpose mechanical parts for typewriters, engines etc.	Transistors, diodes Magnetic heads for tape recorders	Camera shutters Lens holders for cameras and microscopes
Precision machining	5 μm	Mechanical watch parts Machine tool bearings Gears Ballscrews Rotary compressor parts	Electrical relays Resistors, condensers Silicon wafers TV colour masks	Lenses Prisms Optical fibre and connectors (multi-mode)
	0.5 μm	Ball and roller bearings Precision drawn wire Hydraulic servo-valves Aerostatic bearings Ink-jet nozzles Aerodynamic gyro bearings	Magnetic scales, CCD Quartz oscillators Magnetic memory bubbles Magnetron, IC line width Thin film pressure transducers Thermal printer heads Thin film head discs	Precision lenses Optical scales IC exposure masks (photo, X-ray) Laser polygon mirrors X-ray mirrors Elastic deflection mirrors Monomode optical fibre and connectors
Ultra-precision machining	0.05 μm	Gauge blocks Diamond indentor tip radius Microtome cutter edge radius Ultra-precision X–Y tables	IC memories Electronic video discs LSI	Optical flats Precision Fresnel lenses Optical diffraction gratings Optical video discs
	0.005 μm		VLSI Super-lattice thin films	Ultra-precision diffraction gratings

Notes
CCD charge coupled device
IC integrated circuit
LSI large scale integration
VSLI very large scale integration

* - after Taniguchi (1983) by McKeown (1996)

1.2. RESEARCH ACTIVITIES

The rewards for the developments in the field of UPM/UPG are immense. As already mentioned this technology was pioneered by Bryan (1979) of the Lawrence Livermore National Laboratory (LLNL) and McKeown (1987) of Cranfield Unit for Precision Engineering (CUPE) in the U. K. and subsequently put to practice by a number of machine tool builders.

The Japan Society for Precision Engineering (JSPE) founded in 1947, was based on the association of precision machinery, which had been originated by Prof. Tamotsu Aoki in 1933 (Taniguchi 1983). In Japan, the ERATO project (Exploratory Research for Advanced Technology), organized by the Japanese Research and Development Corporation, includes nano-technology as one of the six topics selected for high priority government/university/industry joint development. In the U. K., a National Initiative on Nanotechnology (NINO) was established at National Physical Laboratory (NPL) under the Department of Trade and Industry (Franks 1988).

In the USA, the first ultra precision machine tool was fabricated by Du Pont at the Oak Ridge National Laboratory (ORNL) and operated by Union Carbide in 1962. Since then, there has been a constant advancement in the development of ultra precision machine tools (e.g. Feynman 1961, McKeown et al. 1982, Donaldson 1983, Brown 1983, Ueda et al. 1991, McKeown 1996), to fabricate large and high precision optical, mechanical, and electronic components.

The VHSIC program (Very High Speed Integrated Circuits) in which IBM, Texas Instruments, and other large companies are participating is well under way. The Office of Naval Research (ONR) has sponsored Precision Engineering (PE) programs at several universities. The PE program at LLNL is highly significant. American Society for Precision Engineering (ASPE) has been formed recently. There are seven groups of universities at NBS and in industry who are carrying out significant work in Scanning Tunneling Microscopy (STM) into the atomic domain. The Nanotechnology Experimental Work Station (NEWS) is in the final stages of design at the University of Arizona.

1.3. ADVANTAGES AND LIMITATIONS OF ULTRA PRECISION MACHINING

UPM has several advantages and some limitations over other machining processes (Seo, 1993).

Advantages:

- high form accuracy and repeatability
- moderate material removal rate
- minimum operator skill due to computerization
- no possibility of imbedding foreign materials in the machined surface
- superior local surface roughness as well as global flatness
- relatively large machinable workmaterial surface
- no environmental contamination due to by-products such as chemicals and noises.

Limitations:

- To formulate the mechanism of chip formation in UPM based on experimental work, the chips generated as well as the machined surface need to be examined and correlated with the machining process. When the depth of the material removed is on the order of a few atomic layers, it becomes somewhat difficult and time consuming to study the mechanism of material removal, subsurface damage etc. in actual machining using the ultraprecision machine tools.

- In order to study the effect of cutting conditions and tool geometry, expensive single crystal diamond tools have to be used. Consequently, the cost of experimentation can be significantly high and even then these

experiments can be done only in those laboratories which are equipped with expensive environmental controlled ultraprecision machine tools.

- The accuracy attainable in UPM is dependent upon mechanical movement resulting from the control system and physical tool edge geometry.

In order to overcome some of these limitations and utilize this precise technology it becomes necessary to develop alternate methods and obtain a better understanding of the phenomena of metal cutting at nanometric level. Even though, the technology has paved its way into manufacturing components with dimensional tolerances of a few tens of nanometers, much can be gained by understanding the tool-tip interactions, mechanism of chip formation, deformation mechanisms, energy dissipation etc. at atomic level. This is somewhat limited by the developments in metrology, cost of experimentation, mechanical constraints etc. Computer simulations come as a handy tool in this situation to study UPM in an effective and cost controlled environment.

1.4. COMPUTER SIMULATION

Bacon - "father of scientific philosophy", gave the scientific method consisting of four steps:

1. Observation of a physical system
2. Formulation of a hypothesis (or mathematical model) to explain the observations of the system
3. Prediction of the behavior of the system on the basis of the hypothesis using mathematical models

4. Performance of experiments to test the validity of the hypothesis or mathematical model

Yet at times, it becomes costly (like UPM) or even practically impossible (to form mathematical equations for complex systems) to follow the four steps outlined above. In such a case, some form of simulation may be a satisfactory substitute. The other reasons for using simulation are,

1. It makes it possible to study and experiment with the complex interactions of a given system
2. It is possible to study various effects (for example environmental changes) by making alterations in the model
3. Facilitates a better understanding of the system and consequently assists in improving the design of the system before implementing it
4. Simulations can be used as a pedagogical device for teaching both students and practitioners basic skills in theoretical analysis, statistical analysis, and decision making
5. The knowledge obtained in designing a simulation study frequently suggests changes in the system being simulated which can be studied and tested via simulation before implementing them on actual system
6. Simulations can be used to detect the variables which are important in the system and how the variables interact
7. Computer simulation is convenient way of breaking down a complex system into simpler systems
8. Simulations facilitate the study of dynamic systems in either real time, compressed time or expanded time
9. When new components are introduced into a system, simulation can be used to detect bottlenecks and other problems that may arise in the system

The following is the classification of various simulation models.

1. DETERMINISTIC: Operating characteristics are assumed to be exact relationships rather than probability density functions.

2. STOCHASTIC: At least one of the operating characteristics is given by the probability function.

3. STATIC: These models do not take variable time in to account.

4. DYNAMIC: Models that deal with time varying interactions.

Since the position of the atoms of the tool and the workmaterial during machining vary with time, our simulation models are developed as dynamic models.

1.5. MOLECULAR DYNAMICS SIMULATION

Since the material removal in UPM is on the order of a few atom layers, it is possible to analyze the process by Molecular Dynamics (MD) simulations. MD techniques give higher atomic distance resolution of the cutting process. Consequently, it is possible to study phenomena at nanometer length scale that cannot be attained in a continuum analysis. MD simulations produce a clear picture at atomistic level that gives a microscopic view which is a compromise between analytical models and results from experiments.

MD simulations, however require powerful workstations that can simulate millions of atoms and yet provide results in a reasonable time frame. Initially, due to lack of computational resources, MD simulations were conducted only in some of the national labs (LLNL) equipped with large and powerful mainframes. Today, with the introduction of low cost parallel computers and powerful workstations with fast processors (e.g. Digital Alpha workstation with 333MHz clock speed), it is possible to construct large scale

(50,000 - 1,000,000 atoms) MD computer simulations of nanometric cutting and indentation in research labs.

Using this technique, the response of a material subjected to an external force can be studied. For this purpose, the trajectory of every atom in the material is evaluated by solving the differential equations of motion of all the atoms. An interatomic force model is used to determine the force on each atom due to its neighbors. The mechanism of chip formation and the effects of cutting parameters on subsurface deformation and tool geometry, etc. can be studied without the need for elaborate experimental facilities and costly single crystal diamond tools. Of course, validation of MD simulation results requires selected experimentation. This can be done with the results reported in the literature or selective experimentation.

In Chapter 2, discussion of the works reported in the literature on UPM and studies of UPM using MD simulation are presented. The major disadvantages associated with the limitation of MD simulations of nanometric cutting are significant computational time and memory requirements. In order to overcome these disadvantages, 2-D model of cutting and high cutting speeds (~500 m/sec) are reported in the literature.

In Chapter 4, a brief review of classical mechanics theory used in the MD simulation of nanometric cutting is provided. The formulation of the differential equations used to track the trajectory of atoms and the method adopted in solving the differential equations are presented.

In Chapter 5, a new MD simulation technique called the Length Restricted Molecular Dynamics (LRMD) for nanometric cutting is proposed. In this technique, the length of the workmaterial is maintained constant throughout the experiment but its position is made to shift along the direction of cut, i.e. the atoms from the machined part of the workmaterial

that are not going to affect the simulation results significantly are discarded (or saved separately if need be) but their memory positions are retained. These memory positions are used to add new atoms to the workmaterial. This way the number of atoms considered in the simulation will be considerably reduced and it is possible to move the workmaterial to enable the cutting action to be carried out to any distance even with a smaller initial size of the workmaterial.

In Chapter 6, the results of an investigation carried out using MD simulation to study some of the aspects of machining with negative rake tools are presented. LRMD method was applied in this study. Effect of rake angle on cutting forces, specific energy, subsurface deformation, and size effect were studied by conducting experiments with different rake angles (both positive and negative). The simulation results were compared with the experimental results of Komanduri (1971). An increase in cutting forces, ratio of thrust force to cutting force, specific energy, and subsurface deformation were observed with decrease in rake angle.

CHAPTER 2

LITERATURE REVIEW

2.1. INTRODUCTION TO ULTRA PRECISION MACHINING

Table 1.1 (Chapter 1) identifies the tolerance bands and applications of conventional machining and ultra precision machining. It can be inferred from the table that most of the advanced technology components fall in the micro to nano-regime and hence need to be machined to a high degree of accuracy and finish. This can be facilitated by a better understanding of the material removal process at nanometer level. However, our understanding of material removal mechanisms at such small depths of cut (nm to angstroms) is somewhat limited by technological difficulties in measuring forces and observing chip formation process. In such a situation, MD simulation becomes an alternate tool to study the nanometric cutting process to enable a better understanding of the process. However, the simulation results have to be checked with the results reported in the literature or by selective experimentation. The subsequent sections in this chapter provide a

brief literature review of the experimental and simulation works pertaining to nanometric cutting.

2.2. ULTRA PRECISION MACHINING AT SMALL DEPTHS OF CUT

The technological advances in the design and construction of ultraprecision machine tools were mainly due to the pioneering works of Bryan (1979) of LLNL and McKeown (1987) of CUPE. This has enabled machining of non-ferrous materials using a single crystal diamond tool and grinding of ferrous materials using super abrasives at nanometric level. However, further advances in this field is somewhat restricted by the current state of the knowledge on the physics of machining at very small depths of cut.

In conventional metal cutting, certain zones of energy dissipation can be neglected at large depths of cut (e.g., sliding along flank face of the tool, extended shear zone into the workmaterial, etc.). However, their relative importance may increase when the depth of cut is in the range of nanometers. Nakayama and Tamura (1968) studied the effect of depth of cut on specific energy. They conducted experiments with tool rake angles of 0°, -20°, and -40° with 3 to 4 μm and 17 μm edge radii. They machined brass at 0.1 m/min with the uncut chip thickness ranging from 2 to 40 μm to avoid built-up edge, high temperatures, and strain rate effects. They attributed the plastic flow in the subsurface of the workmaterial to the extension of the shear zone (important energy dissipating zone) below the machined surface at small depths of cut. This energy dissipation was not proportional to the depth of cut but increased rapidly with decrease in depth of cut. An increase in the

specific energy with increase in the edge radii (i.e. increase in the negative rake angle) was also observed. Both decrease in depth of cut as well as increase in negative rake result in a significant increase in specific energy and this increase can be attributed to the size effect. However, they were not able to conduct experiments with tool edge radii < 2 μm at which range subsurface plastic deformation resulting from sliding at the flank face may become predominant.

Furukawa and Morunuki (1988), conducted machining experiments on various workmaterials (e.g. aluminum, germanium, acryl resin) with different grain size and at cutting speeds of 100 m/sec. with depths of cut ranging from 0.5 to 10 μm. A single crystal diamond tool with 0.5 mm nose radius, 0° rake and 2 to 3° clearance was used. They found the specific cutting force for various materials to increase significantly with decrease in depth of cut. They also attributed this increase to the size effect. They pointed that the depth of cut at which size effect takes place (~3 μm) may vary with the combination of workmaterial properties, cutting edge sharpness, and geometry of the tool. Dynamic variation of force was observed at grain boundaries of polycrystalline materials, being caused by different properties of grains and orientation. Single crystal or amorphous materials gave random or little change of dynamic force component.

Moriwaki and Okuda (1989) studied the machinability of copper in ultra precision diamond turning. A transition from chip formation process to rubbing and burnishing was observed to be dominant at submicrometer depths of cut. The depth of cut at which this transition occured was estimated to be 2 - 5 times the tool edge radius. They observed an increase in the specific energy with decrease in the depth of cut. This was attributed to the elasto-plastic sliding at the flank face. This dissipation of mechanical energy is

responsible for determining minimum depth of cut, tool performance, subsurface damage, and workmaterial surface integrity. As the depth of cut becomes the same order as the tool edge radius, the contribution of plowing increases as a result of high negative rake.

Unlike in conventional machining, where shear along shear plane and friction along rake face of the tool dominate, micro machining may involve significant sliding along the flank face of the tool due to the elastic recovery of the workpiece material. Plowing effects may also become important. The partition of thermal energies in ultra precision machining may also be quite different. Lucca et al. (1991) have characterized the regions of energy dissipation in orthogonal ultraprecision machining of OFHC copper and fine grain copper at cutting depths of 10 to 0.1 μm. Plunge cutting of a serrated workmaterial at cutting speeds of 6 m/min for OFHC copper and 7.2 and 107.7 m/min for fine grain copper was carried out. The cutting and the thrust forces were found to decrease linearly with decreasing depth of cut down to about 2 μm. The ratio of the thrust force to cutting force was found to increase with decreasing depth of cut. The authors suggest that a significant fraction of mechanical energy expended in the process is not associated with material removal but rather with redundant plastic work of the workmaterial surface. A substantial increase in the specific energy with decreasing depth of cut was observed. The energy consumed in the shear zone alone was unable to account for the substantial increase in specific energy with decrease in the depth of cut. The authors suggest that in ultra precision machining sliding at the tool-workpiece interface and plowing as a result of the tool edge radius may take on an increased relative importance.

Lucca et al. (1993) conducted experiments with four different tools with 0, -10, -20, and -30 degree rake angles to determine the effect of single crystal

diamond tool edge geometry on the resulting cutting and thrust forces and specific energy. Orthogonal fly cutting of Te-Cu was performed at 7.6 m/min. One series of tests was conducted at 76.2 m/min to examine the effect of cutting speed at small depths of cut. They concluded that cutting speed did not play a role in the resulting forces over the experimental range. The results of the experiments showed that both the nominal rake angle and tool edge profile (effective rake angle) had significant effect on the resulting forces and the energy dissipated over depths of cut from 20 μm down to 10 nm. When the depth of cut was found to be relatively large in comparison with the tool edge profile, the resulting forces and energies were influenced by the nominal rake angle. However, effective rake angle was found to play a predominant role when the uncut chip thickness equals the size of the edge contour.

Lucca et al. (1994) conducted experiments with a single crystal diamond tool with 2.5 degree rake angle and 10 degree clearance angle to investigate the dissipation of mechanical energy during ultraprecision machining over a wide range of depths of cut (20 μm down to 0.01 μm) at a cutting speed of 0.8 m/sec. They observed domination of thrust force and reduction in total cutting force at small depths of cut (0.01 μm). The specific energy calculated from the cutting force was found to increase with decrease in depth of cut. They also report that the tool-workpiece contact length decreases with decreasing thrust force and depth of cut and follow the general trend of thrust force. At small depths of cut, rotation of the thrust force towards the workpiece which corresponds to pure indentation was reported. The authors suggest this process as transition from cutting dominant to plowing/sliding indentation dominant process.

Komanduri (1971) investigated the transition from cutting to plowing when machining with single point tools over a wide range of negative rake angles (up to -85°) to simulate grinding. An increase in the ratio of thrust force to cutting force and side flow of workmaterial with increasing negative rake was observed. He also observed an increase in specific energy with decreasing depth of cut similar to grinding. Chip formation was observed with as high a negative rake as -75° and no chips were obtained at -85°. Width of the workmaterial relative to depth of cut was considered to be one of the important factors controlling chip formation, in addition to rake angle and friction. When the width of the workmaterial was reduced, no chip formation was observed resulting in material removal by ploughing and side spread.

The fine depths of cut used, finite edge radius of tool, low ratio of depth of cut to edge radius, quality of the cutting edge and even minute amounts of wear on the clearance face of the tool add to the complexity of the ultraprecision machining process. From the above discussion it can be stated that, today it is possible to produce very fine chips the uncut chip thickness of which is at the order of 1 nm. These chips can be stably removed in diamond turning of free machining workmaterials using a specially prepared high rigidity, high precision machine tool. The fact that material can be removed at nanometric level is interesting and suggests the necessity to study and analyze the chip removal mechanisms and subsurface damage caused by the process.

Since, the material removed in UPM is on the order of a few angstroms, Molecular Dynamics (MD) simulation is a potential tool for analyzing UPM process. The significant costs and time involved in conducting UPM experiments using diamond tools justify MD simulation as

an alternate approach. One strategy would be to conduct MD simulation first to study the effect of process parameters and compare the results with selective experimentation, thereby reducing the costs involved in UPM.

2.3. INTRODUCTION TO MD SIMULATION

MD simulation studies were initiated in the late 1950's at the Lawrence Radiation Laboratory (LRL) by Alder and Wainwright (1959, 1960) in the fields of equilibrium and non-equilibrium statistical mechanics to calculate the response of several hundred interacting classical particles using the then highly powerful computers available at LRL. Since then, MD simulation has been applied to a wide range of fields including crystal growth, indentation, tribology, low-pressure diamond synthesis, laser interactions to name a few (Dodson 1990, Landman et al. 1990, Hoover et al. 1989, Peploski et al. 1992, Raff 1992, Chang et al. 1993, 1994, Perry et al. 1994, Kim et al. 1994, Brenner et al. 1996) Numerous papers and several books have been written on this topic (Hoover 1986, Raff et al. 1986, Levine et al. 1987, Goodfellow 1990, Allen et al. 1991, Haile 1992). From this point of view, MD simulation is rather a matured field. However, its application to machining has only been of recent origin and only a limited number of research groups are investigating around the world. In the following, research pertaining to MD simulation of machining will be briefly reviewed.

2.4. CURRENT WORKS IN MD SIMULATION

Since the late 1980's, the group at LLNL has conducted pioneering studies on MD simulation of nanometric cutting of copper with a diamond

tool (Belak et al. 1990, 1991, 1994). The observations made in these MD simulations are rather significant in an attempt to understand the mechanism of material removal in nanometric cutting. Belak et al (1995) made computer animated movies of the MD simulation of nanometric cutting which are very informative. This work led other researchers, particularly from Japan (Ikawa et al. 1990, 1991, Shimada et al. 1992-1994 and Shimada 1995, Inamura et al. 1991-1994, Maekawa et al. 1995, to name a few), and recently at Oklahoma State University (OSU) to explore and extend MD simulation to nanometric cutting.

Belak et al. (1990, 1991, 1993, 1994) studied both 2-D and 3-D cutting of copper using embedded atom method for obtaining the potential energy surface at a cutting speed of 100 m/sec. with different edge radii tools and different cut depths. The carbon atoms in the diamond tool were not permitted to move (infinitely hard tool) in the case of cutting copper. While this may appear reasonable as the hardness of copper is only a small fraction of the hardness of the diamond tool, by making it infinitely rigid, the diamond potential is actually not considered. The chip was found to remain crystalline but with a different orientation than the workmaterial. Regions of disorder in front of the tool tip and in the regions in front of the chip are reported. They also report that dull tools (large radii) require larger forces to achieve the same depth of cut as sharp tools. They also confirm the size effect, dependence of specific energy upon depth of cut reported by other researchers (Furukawa et al. 1988, Moriwaki et al. 1989, Lucca et al. 1991).

Belak et al. (1994) also investigated machining of silicon using a diamond tool at a cutting speed of 540 m/sec. where the tool was allowed to deform. No wear of the diamond tool was observed in this study as the cutting times involved were very brief. The authors report that a layer of

atoms from the workmaterial was transferred to the diamond tool. The temperature in the chip was found comparable to the bulk melting temperature of silicon. They also reported that silicon in the chip and the first few layers of the newly cut surface appeared amorphous. They attributed this to the fact that the energy requirements for the transformation of the crystal into an amorphous solid is less than that required to shear the crystal. The authors state that, direct comparison between experimental and modelling results in this case may be difficult because the empirical interatomic potentials may not adequately model the cohesion and plastic deformation taking place in the high pressure metallic phase of silicon.

The work of Ikawa et al. (1990, 1991) and Shimada et al. (1991, 1992, 1993, 1994) and Shimada (1995) of Japan was mainly on 2-D nanometric cutting of copper with a diamond tool. They investigated the effect of minimum edge radius and minimum cut depth on chip formation process, subsurface deformation, and specific cutting energy in two cutting directions of the workpiece, namely, <110> and <121>. Many of their tests were simulated at 200 m/sec. although a few were at 20 m/sec. for comparison.

Shimada et al. (1992) conducted MD simulation of cutting copper with a diamond tool to investigate the size effect. Comparison of the simulation results were made with the experimental results (micro-cutting) as well as that obtained by the simple shear plane model calculations. They reported computational time of 170 hrs. for a cutting distance of 35 nm on 6076 atoms of workmaterial at a cutting speed of 200 m/sec. They observed an increase in the cutting force with increase in the cutting edge radius. This was identified due to the burnishing or plowing force of the cutting edge. When the uncut chip thickness is about half of the tool edge radius, the specific energy was found to exceed the heat of formation of copper. This implies that, a large

amount of energy may be used up to deform the workmaterial around the cutting edge for smaller chip thickness. To analyze the thermal field in micro-cutting, the gradient in the thermal field was scaled so as to coincide with that obtained by continuum thermal conduction theory. The authors state that using this scaling it is possible to study thermal field in metal cutting. However, it still remains a difficult approach to study the heat conduction in metal cutting using MD simulations.

Machine tool performance is the primary factor affecting the ultimate achievable machining accuracy in UPM. The second important factor that determines the attainable accuracy is the depth of cut, also known as minimum thickness of cut (MTC). Shimada et al. (1993) studied the feasibility of applying MD simulations to determine the ultimate attainable accuracy in nanometric cutting. Copper and aluminum workmaterials (5400-8000 atoms) where modelled using pairwise sum of Morse potentials in 2-D simulations. An infinitely hard cutting tool (676 atoms) with a 0^{o} rake and 7^{o} clearance was used in the simulations for cutting one atomic layer of the workmaterial at 200 m/sec. Tools with different edge radii (2, 5, 10 nm) were used in the simulations. When MTC was below 0.2 nm no chips were formed and only when the uncut chip thickness was larger than 0.3 nm chips were formed. MTC was found to increase with increase in the edge radius of the tool. For example, it was 0.6 nm for an edge radius of 10 nm. In the case of cutting aluminum, MTC obtained with a 5 nm edge radius tool was found to be at the same level as that obtained in copper cutting with 10 nm edge radius. As the tool edge radius was increased to 10 nm for cutting aluminum workmaterial an MTC of 1.2 nm was obtained. It was also observed that the ratios of MTC to tool edge radius for cutting aluminum were two times that for copper. The authors propose that the tool-work interaction and resistivity to plastic

deformation of workmaterial as some of the plausible factors affecting the differences in MTC for different workmaterials.

Shimada et al. (1993) also observed the generation and movement of dislocations in the workmaterial. In the region below the chip to be removed, they report complicated elastic and plastic behavior due to indentation of the tool and burnishing of the workmaterial. Once the tool has passed the machined zone, they report recession of dislocations due to elastic recovery. However, considerable distortion in the machined surface remains. From the MD simulation results, the authors conclude 0.5 nm as the ultimate attainable surface roughness in UPM of copper. However, they report that in practice, it is not possible to achieve a MTC below 5 nm. The quality of aluminum worksurface was observed to be worse than that of copper. The easier plastic deformation of aluminum and stronger interaction with diamond are stated as reasons for this poor surface roughness obtained with the aluminum workmaterial.

In subsequent work, Shimada et al. (1994) investigate ultimate attainable surface finish when micro-machining copper with a diamond tool, and estimated the surface roughness to be less than 1 nm. The disordered copper atoms due to plowing of the cutting edge were perfectly rearranged after the cutting tool crossed the machined surface. Hence, a worksurface free from residual distortion is reported in this study. The study was extended to observe the effect of crystalline orientation and grain boundary on surface quality. While cutting polycrystalline materials the nanometric distorted layer was observed to remain on the work surface even under perfect cutting conditions. The authors identify this as due to the dislocation trapping effect of grain boundary. However, the ultimate surface roughness was estimated to be at the same level as that of monocrystalline materials.

Extended work was done by Shimada to determine the ultimate machining accuracy attainable in terms of the behavior of workmaterial atoms (1995). Simulations with a variety of edge radii were performed during this study assuming two dimensional orthogonal cutting of the <111> plane of hypothetical copper and aluminum cut by the <111> plane of a diamond cutting edge. Generation of dislocations due to atoms rearrangement was observed. The atoms rearrange in order to relax the lattice strain when the stored value exceeds a certain level. As a result of successive generation and disappearance of dislocations the chip was observed to be removed stably. After the passage of the tool over the machined surface, the penetrated dislocations into the workmaterial were found to move back towards the surface and finally disappear from the work surface. The movement of dislocations towards the surface is due to relaxation as a consequence of workpiece spring-back. From the results the author states the MTC in microcutting of copper as 1/20 to 1/10 of the radius of cutting edge and a larger MTC for aluminum, which is 1/10 to 1/5 of the radius of the cutting edge. In this study it was also observed that in nanometric cutting the surface of chips removed by small uncut chip thickness was severely oxidized. The author also proposes study of wear mechanism of cutting tool from an atomistic point of view based on MD simulations. In his concluding remarks the author addresses significant computational time and high memory requirements as two important limitations of MD simulation and a necessity to develop a method to overcome these restrictions.

Shimada et al. (1995) conducted MD simulation studies to observe the brittle-ductile transition phenomenon in microindentation and micromachining. An octahedral diamond tool was used to indent a silicon substrate. Tersoff type three body potentials were used to evaluate the forces

between Si-Si and Si-C. The tip was indented into the specimen for a depth of 1.5 nm with a speed of 100 m/sec after which it was moved horizontally at 200 m/sec. The results showed that atoms were densely packed in the outer area and relatively sparse near the tip. No generation and movement of dislocation was seen. The atomic disorder near the tip is due to an amorphous state caused by very high stress and compressive temperature rather than dislocation pile up. As the tip was moved horizontally many cavities like vacancies were observed at regular intervals. The movement of cavities observed is due to the presence of elastic and/or thermal shock waves propagated repeatedly from the tip specimen interface. Also, no crack propagation was observed when the depth of cut was reduced to very small value (less than nanometer scale). As the depth of cut reduces, the potential energy stored in the system becomes very small in magnitude. Consequently, the shock wave cannot supply the necessary energy to initiate crack nuclei or to propagate a pre existing crack and hence, there is no brittle material removal mechanism. Similar simulation studies on microindentation were conducted by Brenner et al. (1996) to observe the interaction and behavior of the diamond tool with the silicon substrate.

Inamura et al. (1991-1994) reported MD simulation under quasi-static conditions where only the change in the minimum-energy positions which are the mean positions of the vibrating atoms were followed. This is done by recording the atom positions at which the resultant force on the atom is zero. They considered only about 400 lattice spacings (34a x 6a x 2a, 'a' being the lattice constant) of a copper workmaterial cut by a sharp diamond tool (assumed as infinitely hard). This should naturally result in significantly shorter computational time than MD simulation although the authors did not report the run times. Unfortunately, because of the fewer atoms used,

interpretation of the results was difficult and not as obvious as in MD simulation.

Inamura et al. (1992) studied the effect of interatomic potential used to model the interactions of the tool and workpiece. Different potentials were used to model the interatomic forces at the interface. Also, the effect of parameters selection for the potential was studied (for example, various D parameters for Morse potential). The investigation also included study of effect of crystalline orientation of the workpiece with respect to cutting direction. Three kinds of workpieces with different orientations (<101>, <100>, <110>) were used in the study. Pairwise sum of Morse potentials and Born - Meyer potential was used in this study. An extremely sharp, infinitely hard diamond tool with 6.3 degrees rake and 5 degrees relief was used to machine copper workmaterial. Atomic motion was prohibited in the z direction and the workpiece was allowed to deform only in the x and y directions. When Morse potential (potential representing chemical activity) was used, swelling up of copper atoms in front of the tool forming successive lumps due to buckling of the workpiece was observed. However, when Born-Meyer potential (potential representing no chemical reactivity) was used shear deformation of the workpiece in front of the tool was observed. This type of deformation is similar to that of macroscale cutting. Thus the importance of using a proper potential to model the interatomic forces between the tool and workmaterial was confirmed through this study.

In this study, the authors also observed that the cutting mechanism differs depending on the crystalline orientation and structure of the workpiece. The deformation of a single crystal workpiece was observed to differ from that in macroscale cutting. The authors attribute this to the material property at the surface which plays an important role. When a

polycrystalline workmaterial was cut, deformation of the workpiece was first observed along the grain boundaries which later propagated into the workmaterial. The authors also observed sudden variations (drop) in the cutting force. This sudden drop in the cutting force was found due to the dislocation movement created by the tool. This is because the force exerted by the tool to create the dislocation far exceeds the force required to move it gradually. This change in cutting force is associated with a change in interatomic energy. During elastic deformation the potential energy increases and then drops when movement of dislocation occurs. This drop in energy should be converted to other kinds of energy to maintain a constant total energy. In most of the MD simulations (including this study) this energy release is assumed to be converted into kinetic energy.

Inamura et al. (1993) conducted MD simulation studies for the evaluation of energy consumption and stress/strain distribution in nanoscale cutting. During cutting at atomic level, elastic and plastic deformation occur alternately. This results in gradual increase in potential energy during elastic deformation and drop in the potential energy during plastic deformation. As a result it is possible to identify the atoms which have caused plastic deformation by monitoring the atom potential energy during cutting. Thus the energy dissipation in nanoscale cutting can be estimated by studying the change in potential energy of each atom during cutting. The authors report that about 52% of the total energy is dissipated in plastic deformation at the primary and secondary shear zones and about 42% in plastic deformation below the tool and about 6% for surface generation. The authors in this study also observed an area of high shear strain around the tool tip and along the rake and under the relief face of the tool. Also, part of the uncut area ahead of the tool was observed to be strained locally in nanoscale cutting. An area of

high tension and shear stress was found to extend from the tool tip to partly along the rake face and under the relief face of the tool. The authors also state the possibility of a mechanism other than simple shearing by yield stress as the shear stress in the shear zone was observed to be lower than the theoretical yield stress. Inamura et al. (1994) also presented a method of transformation from an atomic model (nanometric cutting) to an equivalent continuum (FEM) model (machining).

Maekawa et al. (1995) investigated the role of friction and the mechanism of tool wear in nanometric cutting of copper by a diamond like tool. A new method for reducing the computational time (area restricted molecular dynamics) was implemented in this study. The authors report a reduction in the computational time by a factor of 3 by implementing the new technique. This method is discussed in detail in a subsequent section (2.5.3). In this investigation, the authors report experiencing difficulties due to the high interaction between the work and tool atoms which made it difficult for the work atoms to maintain a crystal structure during machining. The authors report that this phenomenon is equivalent to energy beam processing rather than machining. Also, it was observed that when Born-Meyer potential was used, no chip was produced and the work atoms were extruded towards the right hand side of the workmaterial which arises from the fact that only repulsive forces were considered at the interface. Owing to the uncertainty of the friction at the tool-work interface in nanometric cutting, the interatomic potential, especially the cohesion energy was intentionally altered in the simulation. The tool wear was simulated by reducing the cohesion energy of the carbon atoms. The mechanism of tool wear was identified to consist of interdiffusion of the work and tool atoms, and re-adhesion of the worn particles to the tool. The authors observed a similarity

with macro scale machining in the influence of friction and tool wear in nanometric cutting on the cutting mechanism.

It is clear from the brief literature review that while sound foundation has been laid for MD simulation of nanometric cutting, many of the machining problems at practical cutting speeds are yet to be investigated. Table 2.1 lists few of the main simulation parameters and conditions for some of the recent works reported in analyzing the UPM process by MD simulation technique.

It may be pointed out from table 2.1 that most of the MD simulations reported in the literature uses a 2-D model of cutting (plane stress conditions) with one or two layers in the width direction. Even though, this does not represent the actual conditions, namely, 2-D plane strain conditions or 3-D oblique machining conditions, it is used merely to reduce the computational time. In order to consider the plane strain conditions in 2-D orthogonal machining, the width of the workmaterial must be increased beyond that which has been reported in the literature. When this is done, the number of atoms becomes large and consequently, the computational time and memory usage increase dramatically. It is important to perform simulations that could bring out the 3-D aspects of cutting. Of course when a 3-D model is used for the simulation the size of the workmaterial and hence the number of atoms to be considered becomes significantly large. Also, in the 2-D models reported in the literature, atoms are confined to move in their respective planes and movement of the atom outside the plane is restricted. The interaction of the atom with the atoms in the adjacent plane are not considered and hence the number of pairs of atoms considered is reduced consequently, reducing the computational time. For example, a workmaterial of size 4x30x30 has 16,745 atoms, whereas a workmaterial of size 4x12x30 has 6,863 atoms.

Table 2.1 Summary of the MD Simulation Parameters Used by Various Researchers

Author	Work material	Tool	# Work Material atoms	# of Tool Atoms	Potential Used	Computational time	Memory usage	Configuration
Inamura et al. (1991)	Copper	Diamond tool with 6.3' rake, 5' relief	--	--	Morse Potential and Born-Meyer Potential	_	--	2D
Stower et. al (1991)	Copper	Diamond tool with 0' rake	one layer of material	--	Embedded atom	Obtain length scales in reasonable computer time		2D
Shimada et al. (1992)	Copper	Diamond with 0' rake and 7' clearance 0.5, 20 nm edge radius	1 atomic layer was cut (width), 35 nm length. 6076 atoms	--	Morse Potential	170 hours	--	2D & 3D
Shimada et al. (1993)	Copper	Diamond. 0' rake, 7' clearance, 2, 5, 10 nm edge radius	1 atomic layer width of cut 5400,8000	676,172	Morse Potential	Time Step 1,10fs	--	2D

Belak et al. (1993)	Copper and Silicon	Diamond	--	--	Embedded atom	--	--	2D & 3D
Shimada et al. (1994)	Copper (111) Plane	Diamond (111) Plane, O'rake 7' clearance	5400-8000 1 atomic layer width of cut	172-676	Morse Potential	Time step 10 fs.	--	2D
Inamura et al (1993, 1994)	Copper 6ax34a x2a	Diamond rake of 6.3' and relief 5', extremely sharp edge	--	--	Morse Potential	--	--	2D
Maekawa et al. (1995)	Copper (111)	Diamond with 3nm edge radius	2496	120	Morse Potential	computation time reduced by factor of 3.	--	2D
Shimada (1995)	Copper and Aluminum	Diamond (111)	-	-	Morse potential	Time step of 1, 10 fs	_	2D
Brenner et al. (1996)	Silicon	Diamond	18 layers, Total of 4608 atoms	-	Tersoff and Brenner potential	Time step of 0.5fs	-	3D

With increased number of atoms the number of differential equations of motion to be solved (6N, N being the total number of atoms) increases the consequence of which is significantly increased computational time and memory requirements.

In order to reduce the computational time, the cutting speed is often increased significantly (500 m/sec.), which is many times the practical limit of cutting, namely, about 10 m/sec. To reduce the processing time, fewer atoms are often used for the workmaterial. Such a limitation places restrictions on the type of problems that can be studied. Even with the introduction of concepts of data structures, the run time and memory usage cannot be reduced significantly using conventional methods.

2.5. METHODS TO ENHANCE THE COMPUTATIONAL SPEED

Several methods have been developed to enhance the computational speed in MD simulations. Three of the techniques of interest are the so-called book-keeping technique, the linked-list method, and the area restricted molecular dynamics (ARMD) simulation.

2.5.1. BOOK-KEEPING TECHNIQUE

In the bookkeeping technique (Rentsch et al. 1994), a list of neighboring atoms for each atom (based on cutoff radius) is created. For the force calculations, the neighbor list serves to calculate only the interactions of each atom with its tabulated neighbors. The list must be updated continuously, every few steps as atom positions change. This procedure permits the computational time to be decreased to some extent. When the neighbor list of the bookkeeping technique has to be updated, the complete system is checked for neighboring atoms of each atom. Even though, this method reduces the computational time to some extent the process of completing the

list can be time consuming. However, this method is generally adopted to the MD simulation studies.

2.5.2. LINKED LIST METHOD

In order to overcome the additional computational time involved in refreshing the neighbor list, another technique known as the linked list method (Rentsch et al. 1994) was introduced. The linked-list method is an extension of the bookkeeping technique and avoids the additional computational time in refreshing the list by use of structured simulation space. The simulation space is divided into small volumes, and neighboring volumes of each are tabulated as well. When the neighbor-atom list has to be updated, only the small volumes and those directly surrounding are checked (Allen and Tildesley, 1991). These techniques are generally incorporated in most MD simulations but the problem of long computational time still exits. Also, both these methods do not address the problem faced with significant memory requirements.

2.5.3. AREA RESTRICTED MOLECULAR DYNAMICS

To further reduce the computational time, Maekawa et al. (1995) introduced a method termed Area Restricted Molecular Dynamics (ARMD) which enables a reduction in the computational time. Figure 2.1 is the schematic of the ARMD model (after Maekawa et al. 1995) in which copper (111) workmaterial (2,496 atoms) and a diamond like tool (120 atoms) with 3 nm edge radius were used for the simulation using Morse potential. The

simulation was carried out using a 2-D configuration although the authors point out that it can also be applied for 3-D cutting.

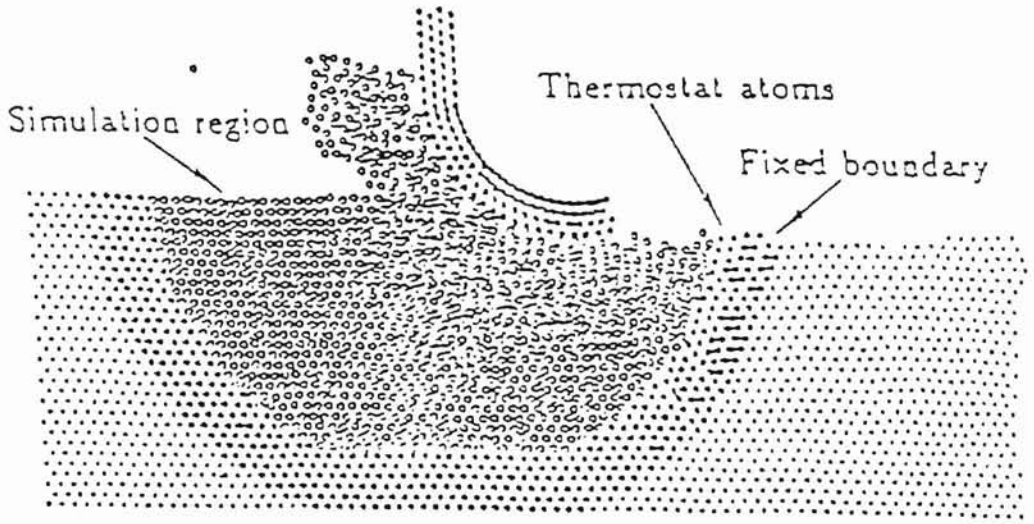

Fig. 2.1 Area Restricted Molecular Dynamics (after Maekawa et al. 1995)

In the ARMD method, the simulation is carried out in a region near the tool nose. The thermostat atoms are placed next to the moving atoms to dissipate the heat generated in the restricted area. A fixed boundary is placed around these thermostat atoms. The radius of the restricted area was chosen to be 7.3 nm. This radius was selected on the basis of accuracy of simulation results in comparison with different radius (e. g. 5.5 nm) for the restricted area. A disadvantage of this method is that, depending on the cutting conditions and tool geometry used, this area has to be modified. The final radius of the ARMD boundary used is based on a comparison of conventional and ARMD results. In other words, both methods must be used

before selecting the restricted area for ARMD simulation. The restricted area around the tool moves along with the tool in the direction of cut. Computation of forces and the potential is focussed only on the atoms which are within the cutoff radius inside this restricted region where atoms are affected by the tool movement.

Using this method, Maekawa et al. reported a reduction in the computation time by a factor of three. However, ARMD does not address the problem of large memory usage. Even though the differential equations of motion are solved only for the atoms inside the restricted zone, the total number of atoms considered in the ARMD method is not reduced. The atoms that do not take part in the simulation are also stored in the memory thereby increasing the memory requirements. Also, the authors point out that the relaxation time for the atoms that are subjected to machining is not sufficient to allow for the elastic recovery of atoms, the consequence of which is more defects remains in the system.

The LRMD technique proposed in this investigation overcomes these limitations. It can perform simulations on larger systems with reduced computational time and memory space requirements. Unlike the ARMD technique, there is no need to conduct comparison MD calculations which can be time consuming.

CHAPTER 3

PROBLEM STATEMENT

It can be seen from Table 2.1 (Chapter 2) that most of the MD simulation work (Inamura et al. 1991, Stower et al. 1991, Shimada et al. 1993, Maekawa et al. 1995) on nanometric cutting was conducted using 2-D configuration, i.e., movement of atoms is confined to a single plane and the interaction of an atom with the atoms in the adjacent plane was not considered. This approach is taken basically to save computational time and memory space requirements. When a 3-D model is used for simulation, the interactions of atoms in adjacent planes need to be considered. Consequently, the total number of atoms considered increases. This results in a significant increase in the number of equations of motion to be solved (6N, N being the number of atoms) and consequent increase in the computational time and memory space requirements. The cutting speeds used for the 3-D simulations has to be very high (100-500 m/sec.) in order to obtain simulation results in a reasonable computational time frame.

It is clear from the literature review, that in order to implement 3-D cutting, cutting speeds closer to practice have to be used in MD simulation studies of nanometric cutting and yet obtain results in a reasonable time frame. One approach is to increase the processing speed using faster computers. The computer manufacturers are constantly improving the processing speeds and that will no doubt facilitate a decrease in the computational time. This will not be adequate and other methods need to be explored in order to conduct MD simulation of nanometric cutting closer to the cutting speeds used in practice. The other alternative which is the focus of this investigation, is to develop simulation techniques that can reduce both the computational time as well as the memory space requirements. In this connection Allen et al. (1987) and Maekawa et al. (1995) have made some significant contributions.

The objectives of the proposed investigation are as follows,

1. To develop an MD simulation technique (known as LRMD simulation) that can be used for 3-D models that will enable a reduction in the computational time and memory space requirements and yet places no restrictions on the cutting process. It is based on the assumption that once the tool has advanced some distance into the workmaterial, the workmaterial atoms in the machined region exert minimal influence on subsequent simulation results (as their interaction with the other atoms will be negligible). Consequently, these atoms are omitted for further simulation and simultaneously a similar number of atoms are added to the leading edge (ahead of the tool) using the memory positions of the discarded atoms. This way, a reduction in both the computational time as well as memory space

requirements can be realized, which will become more significant as the number of atoms considered increases.

2. To validate the results of the new MD simulation technique with conventional MD simulation by comparing the force data as well as the experimental and simulation data reported in the literature.

3. To apply the new MD simulation technique to nanometric cutting with cutting tools of different rake angles (from +45 to -75 degrees) to simulate grinding and also to compare the results of simulation with experimental results of Komanduri (1971). In this investigation only rake angle was varied while maintaining the other cutting conditions, namely depth of cut, cutting speed, work and tool dimensions, a constant.

CHAPTER 4

THEORY OF MD SIMULATION OF NANOMETRIC CUTTING

4.1. INTRODUCTION

Based on the fact that atoms always vibrate around their minimum energy positions and that the minimum energy positions move as the cutting progresses, there are two alternative approaches by which the atomic motion can be described. They are called Molecular Static (MS) analysis and Molecular Dynamics (MD) analysis.

In the first approach, known as Molecular Static (MS) analysis, positions of the atoms at which the resultant force on the atom is zero are recorded and the atoms follow the positions with minimum potential energy. In the second approach, known as Molecular Dynamics (MD) analysis, the position of each atom is obtained by solving Newton's equations of motion

with a high time resolution (smaller than the period of vibration of atoms, on the order of 10^{-15}sec).

4.2. THEORY OF MOLECULAR DYNAMICS ANALYSIS

The principle of MD simulation is the numerical integration of the classical Newton's equations of motion for a system of interacting atoms over a period of time. Classical mechanics describes how physical objects move and how their positions change with time. Its basic laws may be applied to objects of any kind, to solid bodies of any size (above the atomic level), and of any shape and internal structure.

Consider an isolated system comprising N bodies with coordinates (x_i, y_i, z_i) where i=1, 2, 3, ... N (Goldstein 1965). By isolated system we mean that all other bodies are sufficiently remote to have a negligible influence on it. Each of the N bodies is assumed to be small enough to be treated as a point particle. The position of the i^{th} body with respect to a given inertial frame will be denoted by $r_i(t)$. Its velocity and acceleration are given by,

$$\text{Velocity,} \qquad v_i(t) = \dot{r}_i(t) \tag{1}$$

$$\text{Acceleration,} \qquad a_i(t) = \ddot{r}_i(t) \tag{2}$$

Each body is characterized by its mass m_i, a scalar constant. Its momentum p_i is defined as the product of mass and velocity.

$$\text{Momentum,} \qquad p_i = m_i v_i \tag{3}$$

Newton's second law specifies how the body will move. According to Newton's law, force is the product of mass and acceleration.

$$\text{Force,} \qquad F_i = m_i a_i \tag{4}$$

where F_i is the total force acting on the body. This force is composed of a sum of forces due to each of the other bodies in the system. If we denote the force on the i^{th} body due to the j^{th} body by F_{ij}, then

$$\begin{aligned} F_i &= F_{i1} + F_{i2} + F_{i3} + \ldots\ldots\ldots + F_{iN} \\ &= \Sigma F_{ij} \end{aligned} \tag{5}$$

where, $F_{ii} = 0$, since there is no force on the i^{th} body due to itself.

The Molecular Dynamics simulation involve the simultaneous solution of the classical equations of motion for all the atoms. The calculation of classical trajectories involves the numerical solution of an appropriate set of differential equations. The form of these equations depends upon the system potential energy and upon the choice of coordinate system. The trajectories and velocities of the atom are followed over a time period which is often limited by the computational system used.

4. 3. FORMULATION OF THE DIFFERENTIAL EQUATIONS

Consider any two bodies separated by a certain distance one of which is moved away from the other by a distance x.

By Newton's second law, force is the rate of change of momentum.

$$\text{Force in the x-direction} = F_x = \frac{\partial V}{\partial x}$$

$$= \dot{P}_x$$

$$\text{Force in the y-direction} = F_y = \frac{\partial V}{\partial y}$$

$$= \dot{P}_y$$

$$\text{Force in the z-direction} = F_z = \frac{\partial V}{\partial z}$$

$$= \dot{P}_z$$

where, V is the potential of the body.

$$F = ma = \text{first time derivative of momentum}$$
$$= \frac{d(mv)}{dt}$$

Therefore, force in the x-direction,

$$F_x = \frac{d(mv_x)}{dt} = \frac{\partial V}{\partial x}$$

Also, momentum = mass * velocity.

Similarly, momentum in the x-direction,

$$p_x = mv_x$$

By differentiating the equation for the momentum with respect to time, we get the rate of change of momentum.

$$\frac{dp_x}{dt} = \text{rate of change of momentum}$$
$$= \frac{\partial V}{\partial x} \qquad (6)$$

Velocity is time rate of change of distance.

$$\text{velocity in the x direction} = v_x = \frac{dx}{dt} = \frac{p_x}{m} \tag{7}$$

Similarly, the equations in the y and z-directions can be written as,

$$\frac{dp_y}{dt} = -\frac{\partial V}{\partial y} \tag{8}$$

$$\frac{dy}{dt} = \frac{p_y}{m} \tag{9}$$

$$\frac{dp_z}{dt} = -\frac{\partial V}{\partial z} \tag{10}$$

$$\frac{dz}{dt} = \frac{p_z}{m} \tag{11}$$

The potential of the system is calculated using the potential equation. This value is substituted in the equation for momentum (Eqns. 6, 8 and 10) which is obtained by integrating the momentum equation. The momentum value is substituted in the equation for change in position with respect to time (Eqns. 7, 9 and 11) and the position of the atom is determined in the 3-D coordinates. This will provide the trajectory of the atom.

4. 4. NUMERICAL INTEGRATION

The calculation of the trajectory requires the Eqns. 6 and 7 to be integrated numerically from an initial state in the configuration space identified as reactants to some final state associated with products. Some of the frequently used numerical integration methods in trajectory calculations are (Raff et al. 1986) given in the following:

1. Fourth-order Runge-Kutta method (self starting)

2. Fifth, sixth etc. order predictor-corrector methods (non self starting)

3. Variable step size methods

The most frequently used procedure eventually used in this investigation is the forth-order Runge-Kutta method. The Runge-Kutta method attempts to compute the average derivative over the Δx range as shown in Figure 4.1. This average is obtained by computation of the derivative at the start and the end of the interval and twice in the approximate center of the interval.

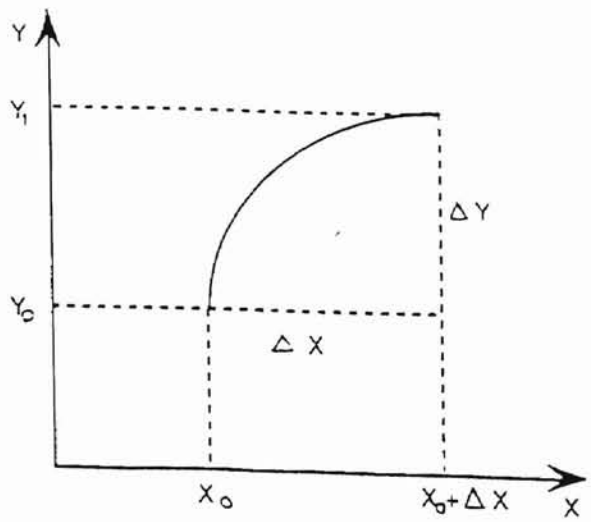

Fig. 4.1 Fourth order Runga-Kutta numerical integration method

The four derivatives are,

$D1 = f(x_o,y_o)$ Start

$D2 = f(x_o+\Delta x/2,y_o+D1*\Delta x/2)$ Center

$D3 = f(x_o+\Delta x/2,y_o+D2*\Delta x/2)$ Center

$D4 = f(x_o+\Delta x, y_o+D3*\Delta x)$ End

The average derivative is approximated as,

$<D> = [D1 + 2*D2 + 2*D3 + D4]/6.0$

from which we compute,

$\Delta y = <D>*\Delta x$ and $y1 = y_o+\Delta y$

The Runge-Kutta procedure has several advantages. First, it is "self-starting" in that it is unnecessary to know the values of the elements at times prior to $t = t_o$. Second, the local error in a given integration step is of a very small order which can be neglected without affecting the results significantly. The method therefore provides good accuracy. Finally, the method is stable and easy to program. The disadvantages associated with the method are its inability to estimate accuracy being achieved during the integration and the number of derivatives (24N) to be evaluated in each integration step. Consequently, the method can be very demanding of the computer time.

In practice, the first disadvantage is not a serious one. An estimate of accuracy during the integration can be obtained by monitoring the computed values of quantities, such as the system energy and angular momentum which are constants. Step size reduction methods and back integration methods are other resources to check the accuracy of the integration results which can be used to overcome the disadvantage stated above.

Predictor-corrector methods have the advantage of providing an automatic error estimate at each integration step, thus allowing the program to employ a variable step size to achieve a specified accuracy. However, these methods are not self-starting. Therefore, it is necessary to use Runge-Kutta method or similar single step method to start the integration. Once started this method has a speed advantage over other methods since only 12N

derivatives must be evaluated in comparison to 24N for Runge-Kutta method. Owing to the greater stability of Runge-Kutta methods, it is sometimes found that a trajectory actually requires fewer derivative evaluations when integrated with Runge-Kutta method than with predictor-corrector procedure, provided similar accuracy is required in both cases. The choice of an integration method thus remains arbitrary.

4.5. INTERATOMIC POTENTIAL

The interatomic potential used in a simulation to model the lattice of the workmaterial and tool plays an important role in determining the accuracy of the simulation results. The complexity of the potential determines the computational time required for the simulation.

Inamura et al. (1992) used two different potentials to consider the interaction between the tool and workmaterial. They used pairwise sum of Morse potential and Born-Meyer potential to model the forces between a copper workmaterial and diamond tool (infinitely hard). From this study they concluded that the cutting mechanism differs depending upon the interatomic potential used in the simulation. In this study the potential which exhibits chemical activity apparently did not create a clear shear plane in the workpiece during cutting, but appears to have caused buckling on the workmaterial surface in front of the tool. A potential which exhibits no chemical activity apparently creates a shear plane in the workpiece. Also, the parameters selected for the potential based on the physical properties of the material being simulated plays an important role in the simulations results.

A brief description of the pair potential used in this simulation to model both the tool and the workmaterial is given below.

4. 5.1. PAIR POTENTIAL

Pairwise interactions are still considered applicable for many atomistic studies and are used in most of the MD simulations.

Pair potentials (Vitek 1996) can be classified into two basic categories based on their contribution to the total energy. In the first type, the potential determines the total energy of the system under consideration, whereas, the second type determines change in energy when the atomic configuration of the system varies under constant density conditions. In both cases, the total energy of the system composed of N particles is given by,

$$E_{total} = \frac{1}{2} \sum_{i\pi k=1}^{N} F_{ik}(r_{ik}) + U(\Omega) \qquad (12)$$

where, Φ_{ik} is the pair potential

r_{ik} is the separation between atoms i and k

U = 0 for first type potentials

Ω is the average density of the material

The simplest and most commonly used form of potential is the Morse potential which is of the form,

$$\Phi(r) = De^{-2\alpha(r-r_0)} - 2De^{-\alpha(r-r_0)} \qquad (13)$$

where, r is the cutoff radius.

The potential has a repulsive term for short separation of atoms and an attractive term to consider the case of intermediate separations. The potential converges to zero at large separation distances.

The constants D, α, and equilibrium atomic distance (r_o), in the equation are determined based on physical properties of the material such as, bulk modulus, rigidity modulus, lattice spacing etc. The energy curve as a function of atomic distance is as shown in Figure 4.2. The values of α, D, cutoff radius (r_{cut}) and the equilibrium atomic distance (r_o) can be used to predict the brittleness/ductility of the material under study. The variation of brittleness with α is as shown in Figure 4.2. The variations of the Morse potential and force value with interatomic distance for different D parameters are as shown in Figures 4.3 (a) and (b) (after Ikawa 1995). The variations of Morse potential and force value with interatomic distance for different values of α are shown in Figures 4.4 (a) and (b) (after Ikawa 1995) respectively.

Lennard-Jones potential is another type of pair potential which is of the form,

$$\frac{\lambda_n}{r^n} - \frac{\lambda_m}{r^m} \qquad (14)$$

Born-Meyer potential is another type of pair potential but only with the repulsive term to consider small atom separation. This type of potential is used in the study where the attractive term plays a minor role, for example in atomic collisions. The functional form of this potential is given by,

$$\Phi(r) = Ae^{-Br} \qquad (15)$$

where, A and B are two adjustable parameters.

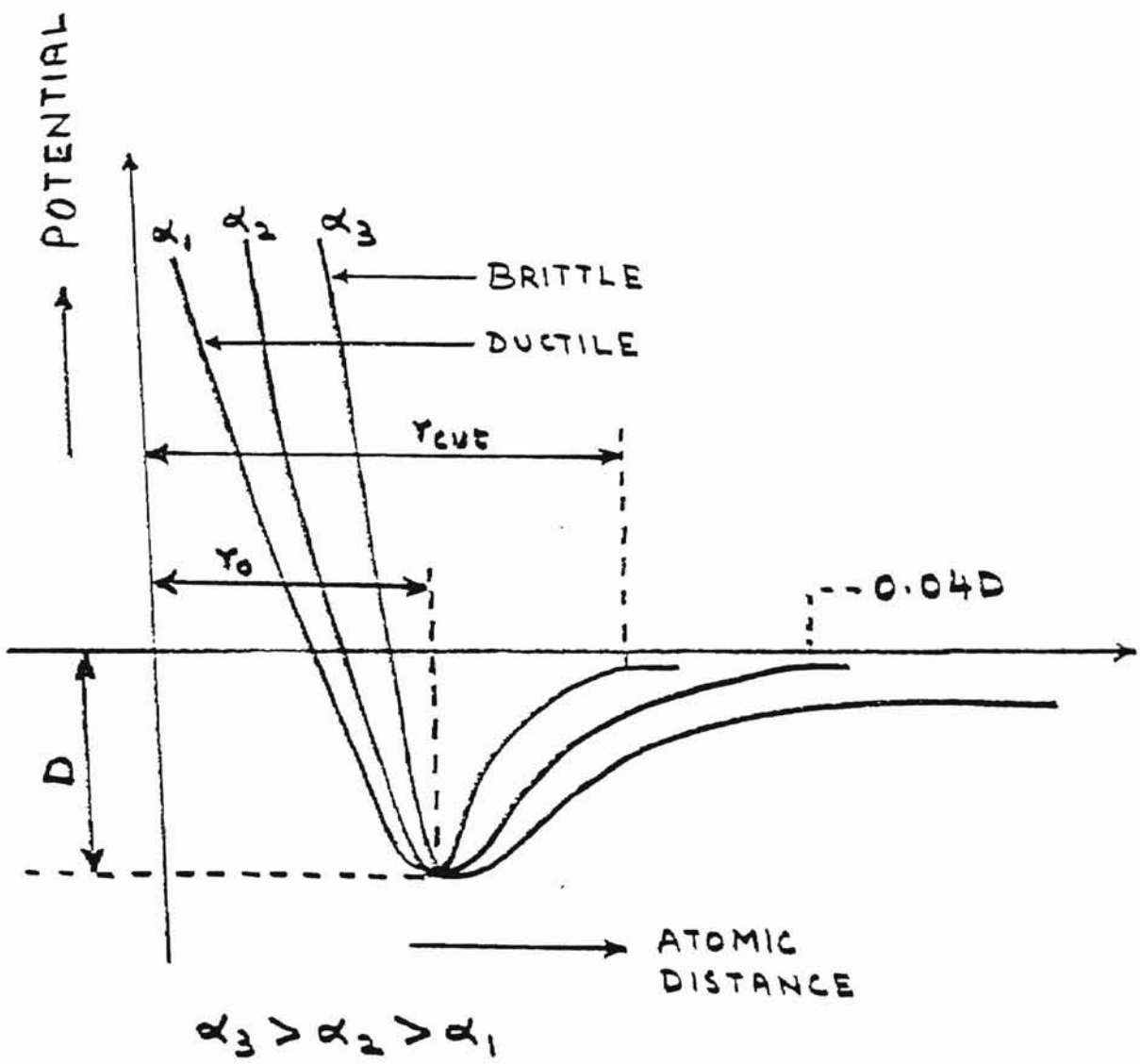

Fig. 4.2 Potential energy curve for pairwise sum of Morse potentials as a function of atomic distance

Pair potentials are most appropriate in the studies of lattice defects in sp-valent metals. They are the simplest form of potentials and hence are used in cases where their use has no physical justification. But the simplicity of the potential and hence reduced computational time increases its use in defining interactions in other materials, especially metals.

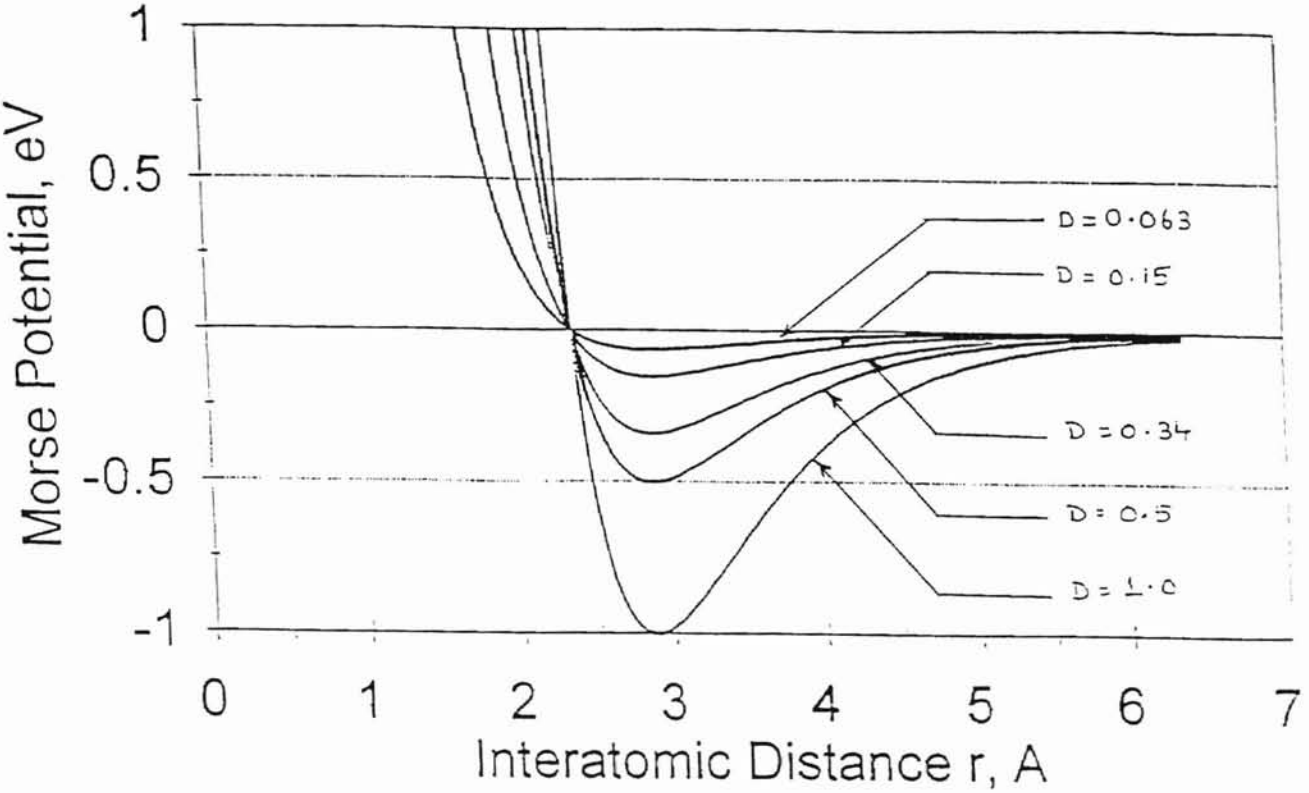

Fig. 4.3 (a) Variation of Morse potential with interatomic distance for different values of D (after Ikawa 1995)

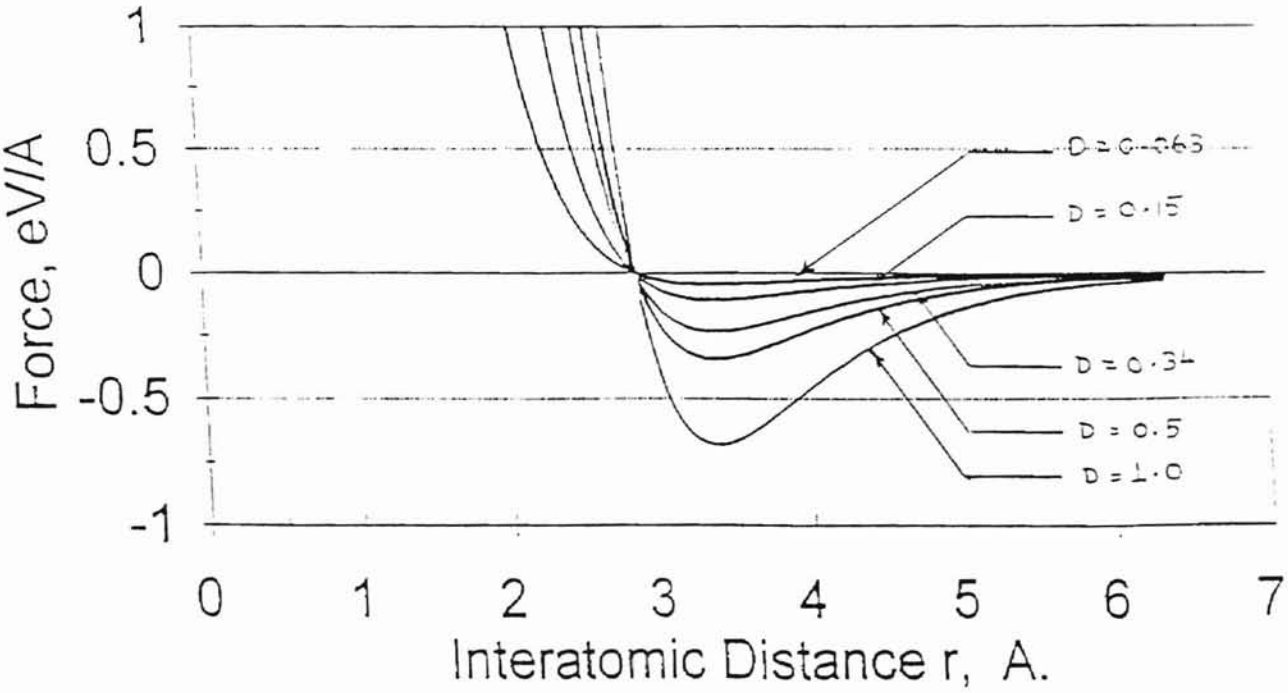

Fig. 4.3 (b) Variation of Force value with interatomic distance for different values of D (after Ikawa 1995)

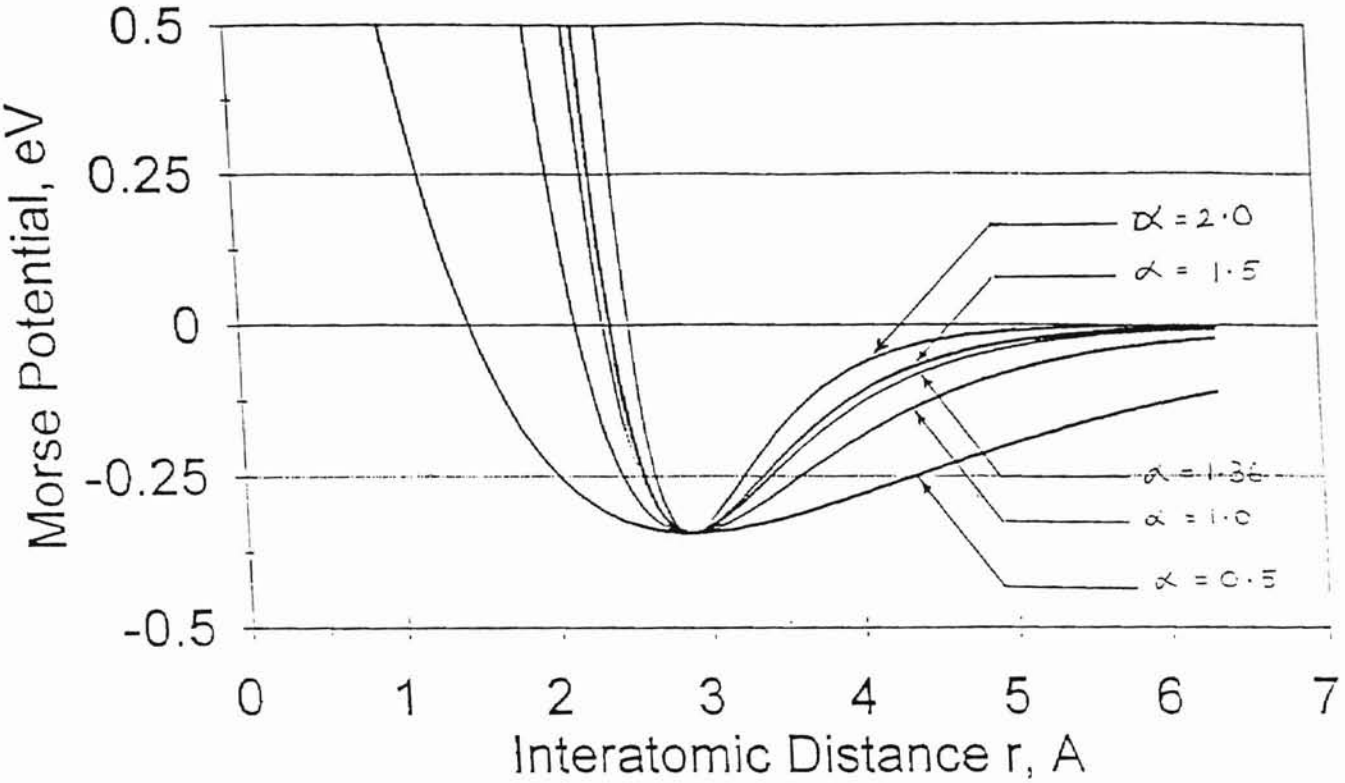

Fig. 4.4 (a) Variation of Morse potential with interatomic distance for different values of α (after Ikawa 1995)

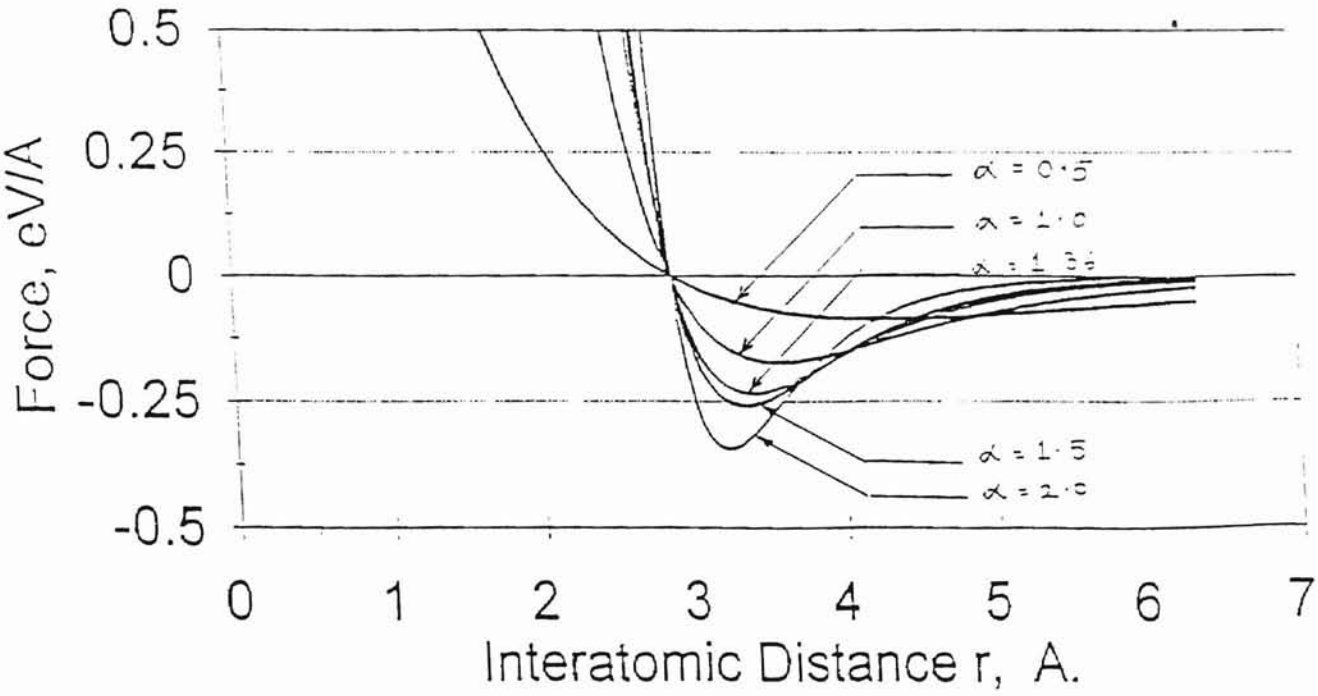

Fig. 4.4 (b) Variation of Force value with interatomic distance for different values of α (after Ikawa 1995)

4 .5 .2. CHOICE OF MODEL

The following are some of the important considerations in setting up the model for any MD simulation.

1. The number of differential equations to be evaluated depends upon the number of atoms considered in the model (6N, N being the number of atoms). Thus a 100 atom model requires the integration of 600 first-order, coupled differential equations. Consequently, the available computer memory space and the acceptable computational time need to be considered before setting up the size of the model.

2. The number of terms in the potential-energy hypersurface need to be considered. For example, for a pairwise interaction potential, the number of terms = N(N-1)/2.

3. Size convergence factor need to be considered as the results should be independent of N.

4. Consideration of a proper dimensionality that would represent the model as close as possible to reality need to be carried out. This is an important point as we need to consider a 3-D model and not a 2-D model simply because of savings in the computational time.

5. Although most of the atoms of the bulk may not directly participate in the process of interest, if there is a large energy absorption or release associated with the process, the bulk atoms will be important as a heat sink. This bulk effect has to be properly modelled into the system.

CHAPTER 5

LENGTH RESTRICTED MOLECULAR DYNAMICS

5.1. INTRODUCTION

The first approach towards a reduction in the computation time and the required memory space is to reduce the size of the workmaterial and hence, the number of workmaterial atoms. Once the number of workmaterial atoms is reduced, the number of equations to be solved will be correspondingly reduced, and consequently the amount of memory space required for storing the atoms as well as the computational time will be reduced. However, a major consideration in reducing the number of workmaterial atoms is the effect of workmaterial size on cutting performances. Reducing the workmaterial size will affect the cutting length and may result in distorting the cutting phenomena for which the study is carried out. Another approach commonly practiced to reduce the computational time is to increase the cutting speed. Until the computational

speeds are increased by 2 to 3 orders of magnitude than the current state of the art technology, one has no choice but to use higher cutting speeds (100-500 m/sec) while conventional cutting speeds are in the range of 1-10 m/sec.

A small contribution towards reduction in the computational time and memory requirements is the LRMD in which the workmaterial length is maintained constant throughout the simulation, but, the workmaterial keeps moving along the direction of cut.

5.2. MD SIMULATION CONDITIONS FOR NANOMETRIC CUTTING

MD simulations were conducted using the conventional method as well as the new approach using LRMD. The basic function of the C code on which modifications were made to implement LRMD is explained in Appendix 1.

A Digital alpha workstation (Model 250) with a clock speed of 333MHz was used in this investigation. Copper workmaterial and tungsten tool (hypothetical hard tool) with a 5^{o} rake and 5^{o} clearance angle were used in this simulation.

Simulations were carried out for different cutting lengths, depths of cut, cutting speed, and different workmaterial lengths. Workmaterial dimension was selected based on the length of cut and simulation method. Tables 5.1 and 5.2 give details of the workmaterial and tool, depth of cut, cutting speed (500m/sec in all simulations) and length of cut for conventional and LRMD simulations respectively.

Table 5.1 Details of the Workmaterial and the Tool for Conventional MD Simulation of Nanometric Cutting

Expt. No.	Length of cut (Å)	Workmaterial dimensions	Tool dimensions	Total workmaterial atoms	Total tool atoms	Depth of cut (Å)
1	50	4x16x12	4x10x12	3,713	1,040	7.24
2	75	4x23x12	4x10x14	5,288	1,202	7.24
3	100	4x30x14	4x10x14	7,961	1,202	7.24
4	125	4x35x14	4x10x14	9,266	1,202	7.24
5	110	4x30x30	4x10x14	16,547	1,202	3.62

Table 5.2 Details of the Workmaterial and the Tool for LRMD Simulation of Nanometric Cutting

Expt. No.	Length of cut (Å)	Workmaterial dimensions	Tool dimensions	Total workmaterial atoms	Total tool atoms	Depth of cut (Å)
1	50.0	4x12x12	4x10x12	2,813	1,040	7.24
2	75.0	4x15x12	4x10x14	3,488	1,202	7.24
3	100.0	4x18x14	4x10x14	4,829	1,202	7.24
4	125.0	4x18x14	4x10x14	4,829	1,202	7.24
5	110.0	4x15x30	4x10x14	8,510	1,202	3.62

Table 5.3 gives the computational parameters used in the LRMD simulation. It may be pointed out that while MD simulation of nanometric cutting is presented here, the approach can also be used for other MD simulation problems involving large number of atoms.

Table 5.3 Parameters Used for LRMD Simulation of Nanometric Cutting

Configuration	3-D cutting
Workmaterial	Copper, lattice constant 3.62 Å
Potential used	Morse potential
Morse potential parameters	D = 0.3429 eV, alpha = 1.35588 $Å^{-1}$, r_o = 2.6260 Å, and rcut = 5.74 Å
Tool material	Infinitely hard
Uncut depth	1-2 atom layers
Tool nose radius	sharp edge
Tool angles	5 deg. rake and 5 deg. clearance
Cutting speed	500 m/sec
Bulk temperature	293 K

It can be seen from Tables 5.1 and 5.2 that the total number of workmaterial atoms considered for a particular length of cut is reduced by a significant value when LRMD is applied. For example, from Tables 5.1 and 5.2, for a cutting length of 75 Å by conventional method 5,288 atoms are considered in the workmaterial (4*23*12) whereas only 3,488 atoms are

considered in the workmaterial (4*15*12) when LRMD is applied. It will be shown in this study that both the computational time and memory space can be reduced significantly by LRMD. The validity of LRMD was verified by comparing the force data generated in nanometric cutting by the two methods.

5.3. PRINCIPLE OF LRMD

Figure 5.1 is a schematic of the model used for the MD simulation of nanometric cutting showing various regions of interest.

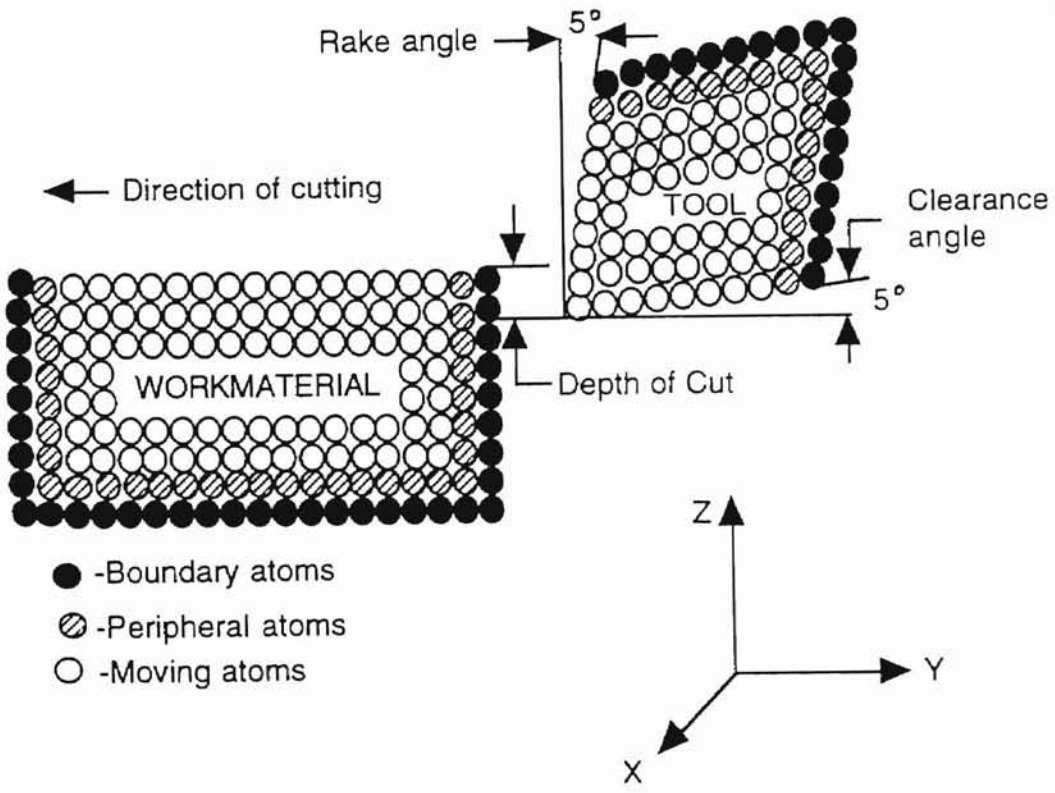

Fig. 5.1 Schematic of MD simulation of nanometric cutting showing various regions of interest

The workmaterial is divided into three different zones, namely, the moving zone, the peripheral zone, and the boundary zone. These zones have also been termed as B-zone, Q-zone and P-zone, respectively (Riley et al. 1988). The motion of the atoms in the moving zone are determined solely by the forces produced by the interaction potential and the direct solution of the classical Hamiltonian equations of motion (Eqns. 6-11). The movement of the peripheral atoms calculated from the Hamiltonian's equations are modified by the presence of the velocity reset functions associated with each atom in the peripheral zone. The boundary atoms are fixed in position. These sites serve to reduce edge effects and maintain the proper symmetry of the lattice.

The velocity reset functions that operate upon the atoms in the peripheral zone serve to represent the bulk effects upon the energy transfer that would be present for an extended lattice model. Various velocity reset methods have been proposed and used successfully by Agrawal et al. (1987) and by Riley et al. (1988). The latter of these is the more general case in that the procedure permits statistical fluctuations about the equilibrium temperature. Under certain conditions, the method can also be shown to be equivalent to a Langevin procedure.

The velocity reset function used in this investigation is of the form (Riley et al. 1988),

$$v_{X_i}^{new}(t_n) = (1-w)^{1/2} v_{X_i}^{old}(t_n) + w^{1/2} v^r(\xi,T) \quad , \tag{16}$$

where $v_{X_i}^{new}(t_n)$ is the new x-component of velocity for atom i at time t_n and $v_{X_i}^{old}(t_n)$ is its old velocity. $v^r(\xi,T)$ is a random velocity selected from a Boltzmann distribution at temperature T by the random number ξ. w is a

parameter that controls the strength of the reset. That is, w=0 corresponds to no reset while w=1 gives a complete reset in which the system retains no memory of its old velocity. Analogous equations are used for the y and z components of velocity. This reset procedure is applied to every atom in the peripheral zone at equally spaced time intervals Δt. Riley et al. (1988) have shown that in the double limit as w --> 0 and Δt --> 0, the equations of motion of the peripheral-zone atoms reduce to Langevin form with a frictional damping rate equal to $w/2\Delta t$.

Riley et al. (1988) recommended that Δt be approximately 1/5 of the Debye period of the lattice. The reset parameter is given by

$$w = pD t \omega D \Gamma_p / 3 , \qquad (17)$$

where ωD is the Debye frequency for the lattice and Γ_p is the ratio of the number of bonds that a Q-zone atom has to the P-zone to the total number of atoms of a bulk lattice atom.

The LRMD method is based on the assumption that once the tool has advanced into the workmaterial through a distance Δx, the workmaterial atoms in the machined region will exert minimum influence upon future simulation results since their interaction with the tool atoms will be negligible. Consequently, one can omit all atoms in the region Δx without significantly affecting the results of the calculations. If desired, the positions of the discarded atoms may be retained. As atoms within the cut region Δx are omitted, we simultaneously add a similar number of atoms at the leading edge of the peripheral zone.

Figure 5.2 is a schematic of the proposed LRMD simulation showing the regions of interest for the exchange process. 'pe' and 'ne' in Figure 5.2

represent the y (+) and y (-) boundaries of the workmaterial undergoing MD simulation of nanometric cutting. The atoms to the right of 'pe' and to the left of 'ne' are the boundary atoms and by definition, are not affected during the simulation. The atoms between 'bb1' and 'pe' are the atoms to be discarded and whose memory positions (index) are used to add new atoms to the leading edge of the workmaterial. The atoms between 'zz' and 'ne' are the atoms whose coordinates are used to add new atoms to the workmaterial. Although, in the following discussion we consider the atoms along the workpiece length, it should be understood that we actually consider the atoms in 3 dimensions (i.e. width and thickness of the workpiece as well).

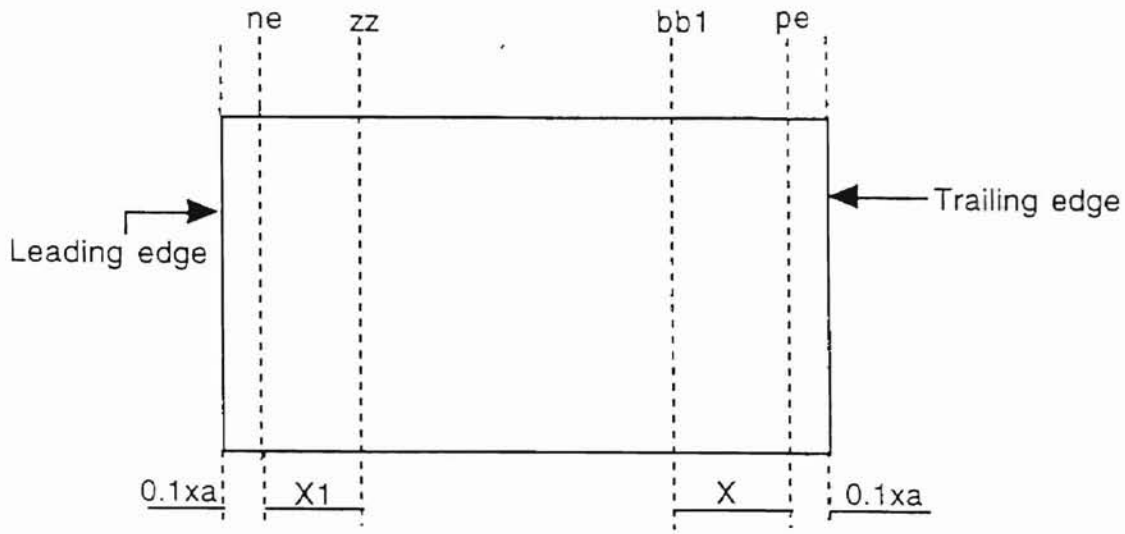

Fig. 5.2 Schematic of proposed LRMD simulation illustrating regions of interest for the exchange process

Initially the number of layers to be discarded from the trailing edge and replaced at the leading edge is chosen, to any desired value and initialized. Based, on this number, the length of the workmaterial to be discarded from the trailing edge after machining is determined (X). This length 'X' is discarded each time the exchange procedure is executed for shifting the workmaterial in the direction of cut. From the leading edge of the workmaterial, the coordinates of the atoms between 'ne' and 'zz' corresponding to a length 'X1' (which is also equal to length X) are stored in a separate array. This process of storing the coordinates of the atoms is carried out prior to the tool advancement into the workmaterial. Consequently, the atoms stored from length 'X1' have the same x and z coordinates as their counterparts in length 'X' but with different y coordinates. In principle, atoms from any part of the workmaterial can be stored for the exchange process with the constraint that the number of layers stored for the exchange process should be the same as the number of layers to be replaced. However, in practice the exchange process and hence the code written to implement LRMD can be simplified if the length 'X1' is selected next to the boundary layer along the leading edge. It should be noted that for the exchange process only the coordinates of the atoms and not the atoms themselves between 'ne' and 'zz' are used. The coordinates of the atoms for the exchange process are not stored for each step, instead the same coordinates are used incrementally as the workmaterial shifts in the direction of cut.

Once the tool has moved through some distance into the workmaterial after which the interatomic forces between the atoms to be removed from the trailing edge of the workmaterial and the tool becomes insignificant, the LRMD method is applied i.e., the procedure for shifting of workmaterial is carried out.

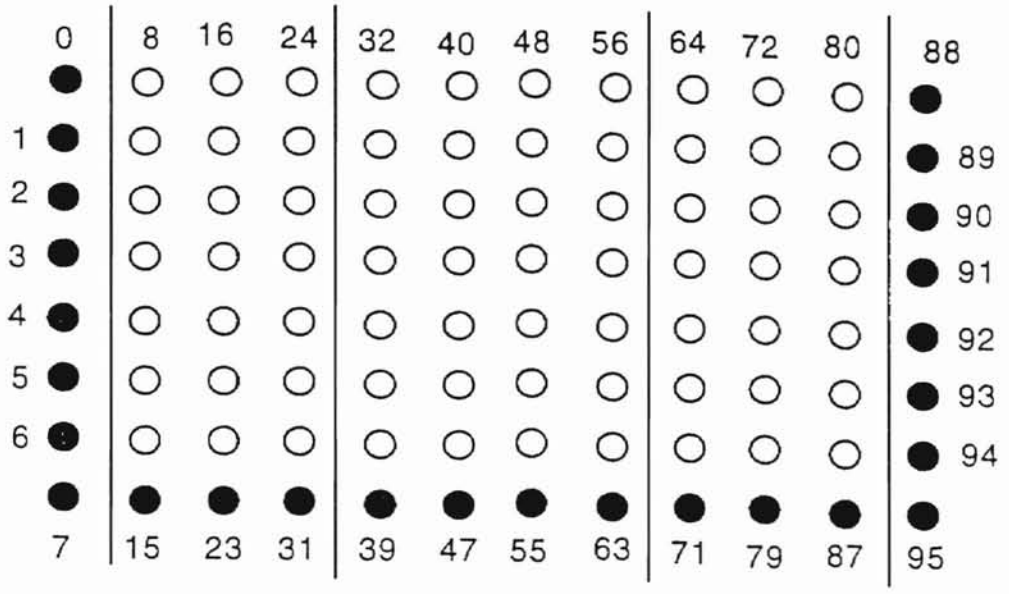

Fig. 5.3 Schematic showing the atom positions considered in the workmaterial before nanometric cutting

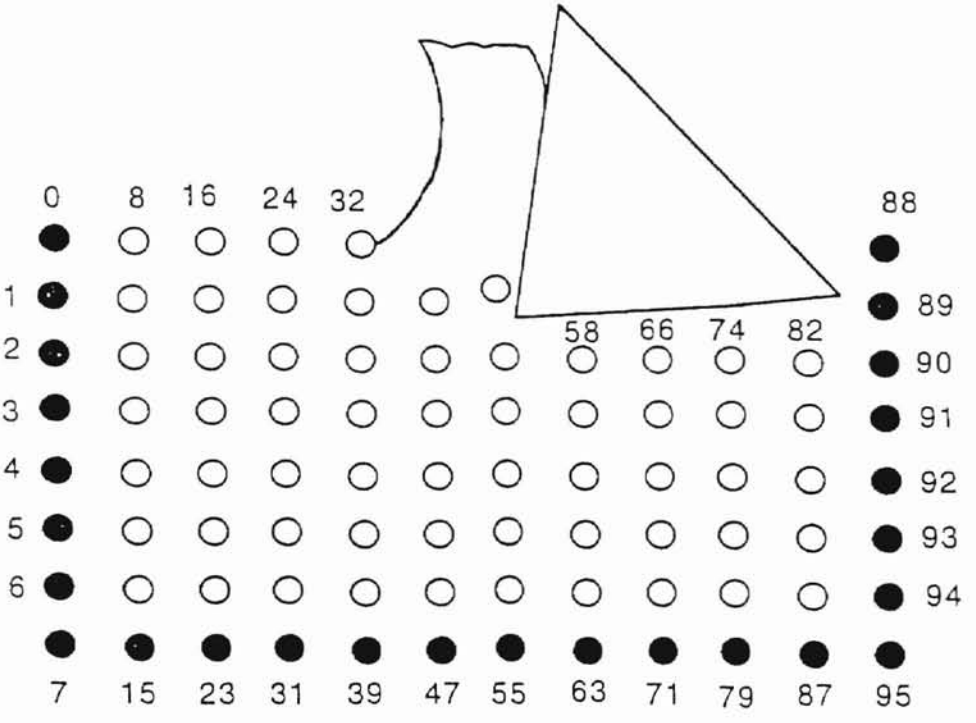

Fig. 5.4 Schematic of workmaterial and tool after the tool has advanced a certain distance into the workmaterial

Figure 5.3 gives a schematic representation of the atom positions in the workmaterial. Figure 5.4 shows the atom positions in the workmaterial after the tool has advanced into the workmaterial.

The boundary layers to the left of "ne" (Figure 5.2) are moved by a distance equal to the length 'X' to be exchanged from the trailing edge of the workmaterial as shown in Figure 5.5.

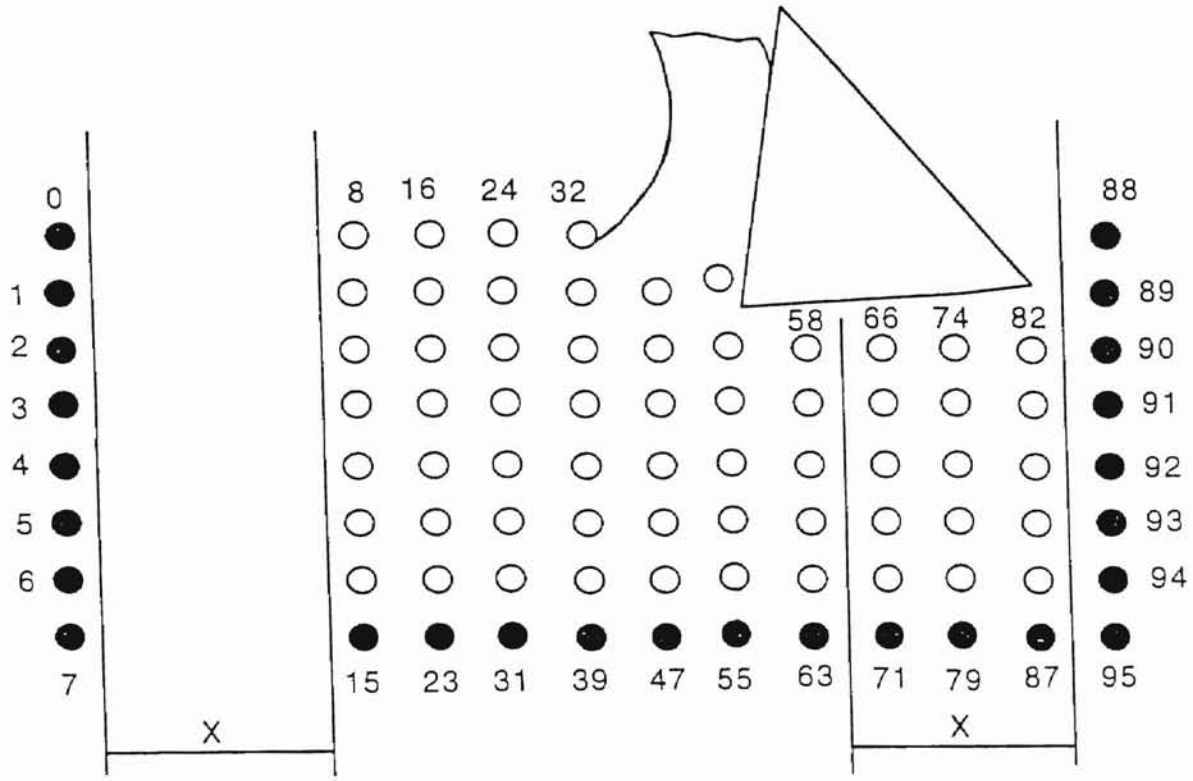

Fig. 5.5 Schematic showing the workmaterial after the boundary atoms along the leading edge of the workmaterial have been moved by a distance equal to the number of layers to be exchanged from the trailing edge

Consequently, there is an empty space between the boundary layer along the leading edge and the moving atoms, the length of which is equal to the number of layers to be added to shift the workmaterial along the direction of

cut. Since, the atoms between 'bb1' and 'pe' (Figure 5.2) do not significantly affect the simulation results (as they constitute the machined surface and will not participate in the cutting process), these atoms are either discarded or stored separately. Discarding here implies that the coordinates of the atoms to be discarded are replaced with new coordinate values (stored in a separate array) which represent new atoms but with the same index. As new atoms are added, the atoms in the peripheral zone advance into the moving zone. These atoms should be corrected for their type (viz. either moving atoms or peripheral atoms as the case may be), as the velocity of the peripheral atoms is reset every one fifth of the time step (0.1 atomic time unit). After the exchange process is executed the atoms of the workmaterial are checked for their type (either moving or peripheral). If an atom is found to be of a different type than prior to the exchange process, then the atom is removed from the old list and added to the corresponding new list (either moving atoms list or peripheral atoms list). Similarly, care should be taken not to include the boundary atoms inside the moving region.

To add new atoms to the leading edge, the coordinates of the atoms stored in the array prior to nanometric cutting (i.e., after the relaxation when they are in the equilibrium condition) are used. The new atoms to be added to the leading edge will have the same x and z coordinates but their y coordinates will be different from their initial stored values. It may be noted that the atoms coordinates between 'bb1' and 'pe' (Figure 5.2) cannot be used for the exchange process as they are in the deformed condition and hence, will disturb the equilibrium of the workmaterial, if used. So, the index of these atoms and not their coordinates is used.

The coordinates of the atoms stored in the array, which represent the atoms inbetween 'zz' and 'ne' (Figure 5.2) are used to add new atoms to the

leading edge. The y coordinates of the atoms stored in the array are incremented by the same distance by which 'ne' is incremented. Thus we have a copy of the atoms between 'ne' and 'zz' with different y coordinates so that they fill up the space created by moving 'ne'. Even though, these added atoms have new y coordinates and are considered as new atoms, they are still identified by the old index of the discarded atoms in which they are stored. Thus the memory location used is the same but the coordinates stored in these locations are different.

It may be noted that even though the lengths 'X1' and 'X' are equal, the number of atoms in these two lengths after machining will not be the same. The number of atoms between 'bb1' and 'pe' will be less than the number of atoms between 'ne' and 'zz' because some of the atoms between 'bb1' and 'pe' have transformed into the chip due to cutting and their positions cannot be used to create new atoms as we may need them for further investigation (chip removal mechanism). In such a case new positions (index) are needed to add some of the additional moving atoms that do not have a previous index to be stored in. By using new index values, the number of moving atoms are going to increase with each exchange process. Even though the number of moving atoms increases, the length of the workmaterial remains constant and this increase in number of atoms is insignificant.

From Figure 5.5 atoms 66 through 87 are not going to affect the simulation results significantly as explained earlier. So, these atoms are removed and new atoms are added to the leading edge using their positions. Since, some of the atoms in the length 'X 'have gone into the chip, some new atom positions need to be added to the leading edge as indicated by atoms 96 through 101 in Figure 5.6. The situation after replacing the new atoms (new coordinates in old index) to the leading edge (ahead of the tool) of the

workmaterial is shown schematically in Figure 5.6. The trailing edge boundary atoms (88 through 95) can also be moved through the same distance 'X' and placed as a boundary in front of atoms 58 through 63.

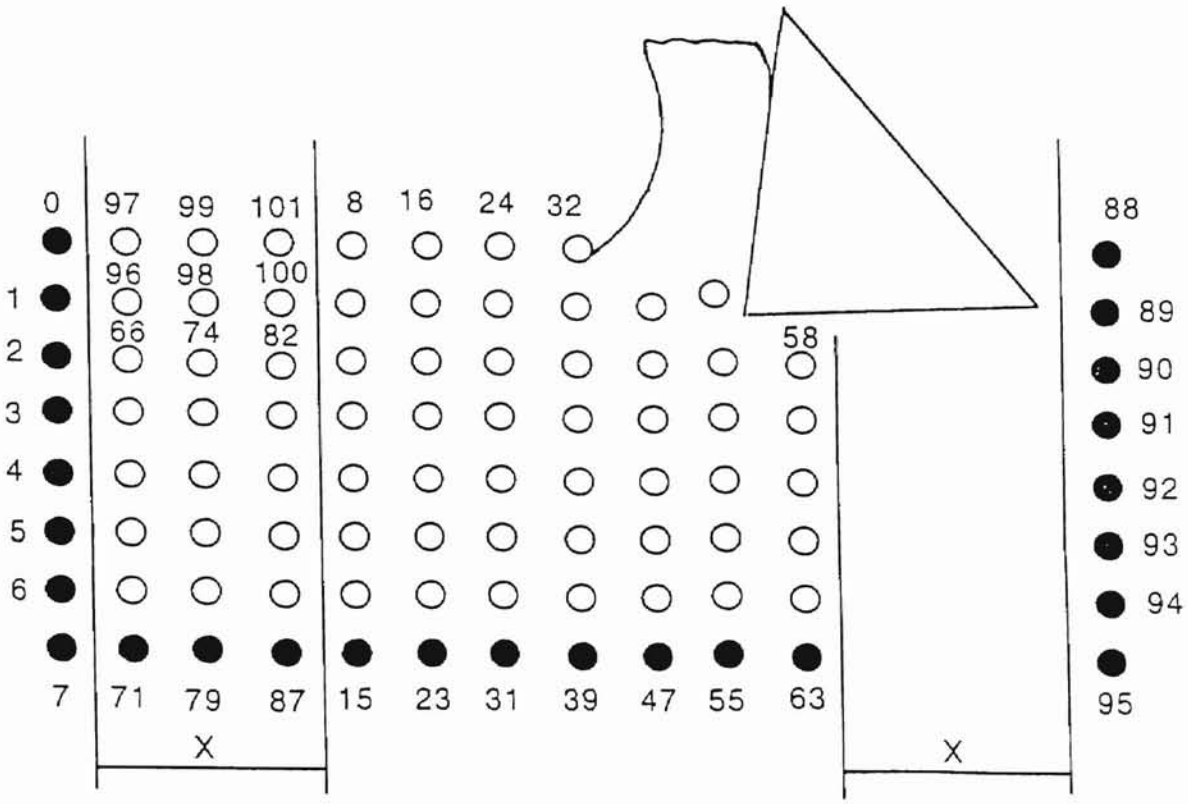

Fig. 5.6 Schematic of the workmaterial after replacing new atoms to the leading edge of the workmaterial

Once the exchange process is complete the boundaries 'bb1', 'pe', 'zz', and 'ne' are incremented by a length equal to the length of workmaterial discarded (X) after which the tool again commences cutting. The runtime required for performing this exchange process is insignificant (a fraction of the time step). By repeating this procedure in a loop it is possible to move the

workmaterial to enable the cutting action to be carried out to any distance even with a smaller initial size of the workmaterial.

5.4. RESULTS AND DISCUSSION

Nanocutting was performed on copper workmaterial using an infinitely hard tool (tungsten). Simulation was carried out for different cutting lengths, depths of cut, and cutting speed. In conventional method as the cutting distance increases the workmaterial length and hence the number of atoms increases. Both computational time and required memory space increase with the total number of atoms considered for simulation. It can be seen from Table 5.4 that they are of significant magnitude.

Table 5.4 Comparison of Conventional MD and LRMD Simulation Methods

Expt. No.	Method	Length of cut (Å)	Workpiece dimension (units)	Tool dimension (units)	Workpiece atoms	Tool atoms	Computa-tional Time (H/M/S)	Memory used by workpiece (bytes)
1	Conv.	50.0	4x16x12	4x10x12	3,713	1,040	4:16:29	397291
	LRMD	50.0	4x12x12	4x10x12	2,813	1,040	3:02:57	300991
2	Conv.	75.0	4x23x12	4x10x14	5,288	1,202	11:32:38	565816
	LRMD	75.0	4x15x12	4x10x14	3,488	1,202	6:39:09	373216
3	Conv.	100.0	4x30x14	4x10x14	7,961	1,202	29:10:16	851827
	LRMD	100.0	4x18x14	4x10x14	4,829	1,202	13:49:30	516703
4	Conv.	125.0	4x35x14	4x10x14	9,266	1,202	43:18:05	973145
	LRMD	125.0	4x18x14	4x10x14	4,829	1,202	17:52:28	516703

In the case of LRMD as the workmaterial shifts its position along the cutting direction it is possible to specify a workmaterial of smaller length and yet perform simulations for greater length of cut. By reducing the workmaterial size a significant reduction both in computational time and memory space is achieved as shown in Table 5.4.

Figures 5.7 (a) to (e) are photographs of the LRMD simulation showing various stages of cutting copper with a hard tool (tungsten). The indentation of the tool into the workmaterial, extensive plastic deformation of the workmaterial ahead of the tool in the primary shear zone, and subsurface deformation in the machined surface can be clearly seen. Figure 5.7 (d) and (e) show the progress of cutting just prior to and after the application of LRMD technique, i. e. the procedure of shifting the atom positions of the workmaterial from the trailing edge (machined surface) to the leading edge of the workmaterial. It can be seen that the process continues smoothly. Figure 5.8 shows the variation of cutting and thrust force with time. The mean cutting force was 33.253 eV/Å (3.679×10^{-2} N/mm) and the mean thrust force was 24.552 eV/Å (2.716×10^{-2} N/mm). The ratio of the cutting to thrust force is 1.3543 which is on the same order of magnitude as in conventional machining. Figure 5.9 shows the results of the variation of the cutting force per unit width versus the depth of cut obtained from the literature (both experimental and simulation data). Also shown in the figure are the data obtained for a cutting depth of 0.724 nm by conventional MD and LRMD methods. It can be seen from Figure 20 that the simulation results by both conventional and LRMD methods are in line with the data available in the literature.

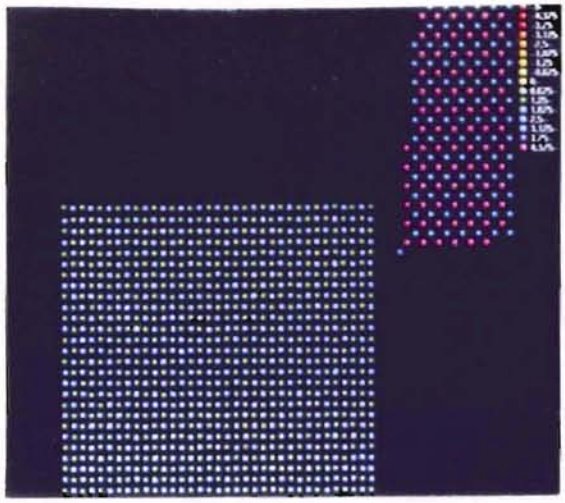

5.7 (a)

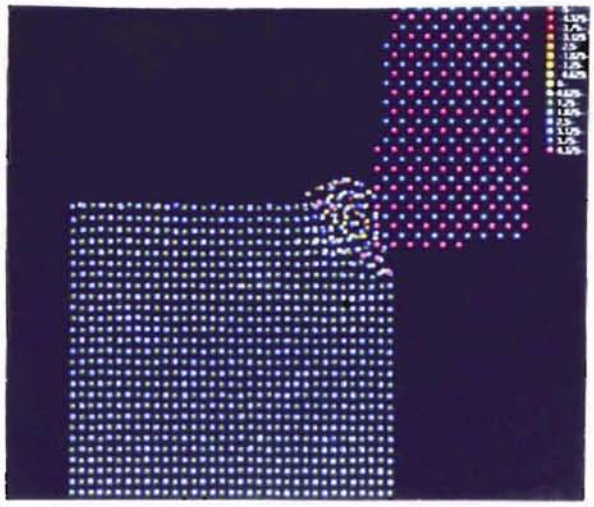

5.7 (b)

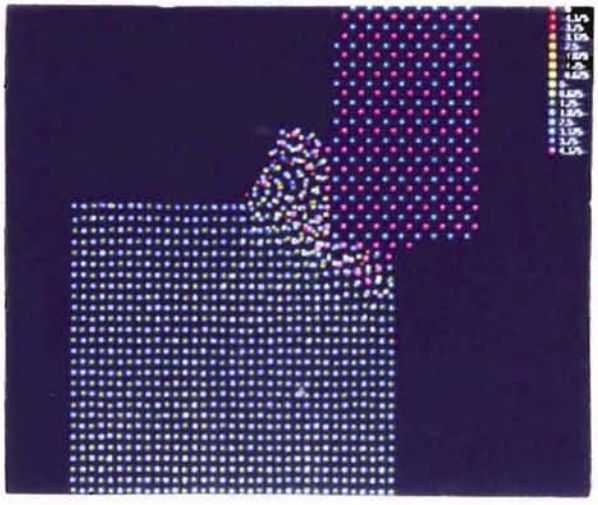

5.7 (c)

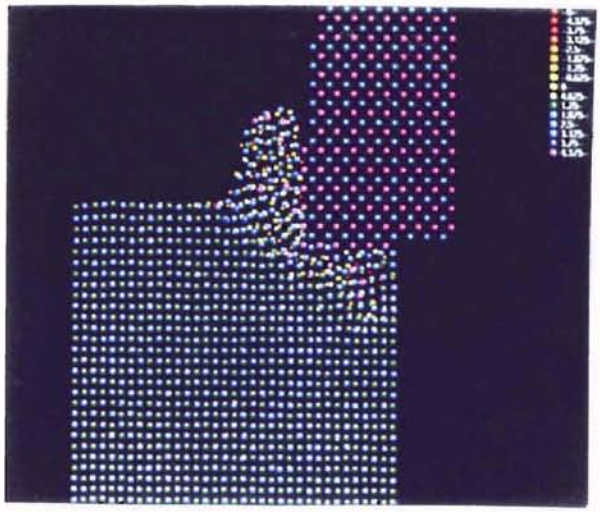

5.7 (d) Photograph of the nanometric cutting process prior to exchange (before LRMD is applied)

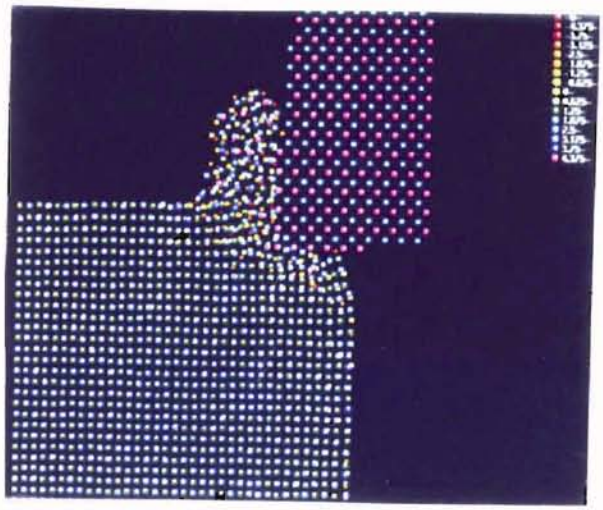

5.7 (e) Photograph of the nanometric cutting process after exchange (after atoms are replaced from trailing edge to leading edge)

5.7 (a) - (e) Photographs of LRMD simulation at various stages of nanometric cutting

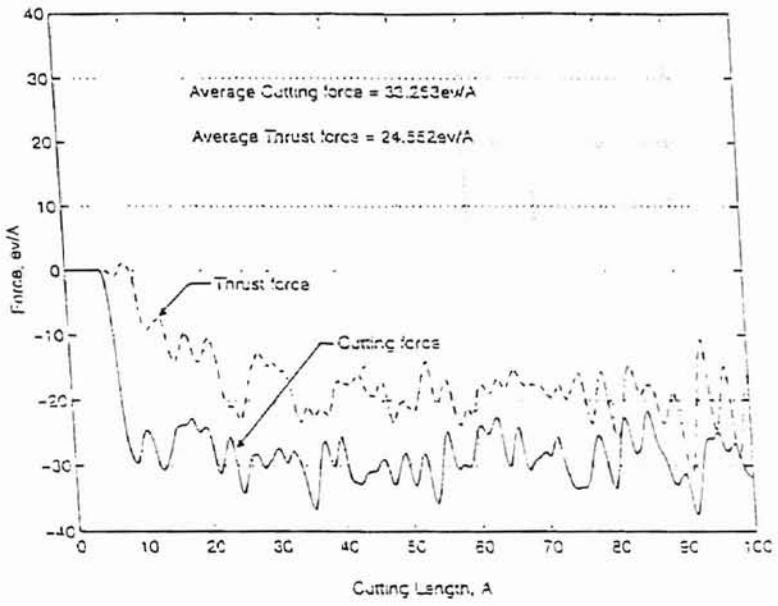

Fig. 5.8 Variation of cutting and thrust force with time by LRMD technique of cutting copper with a hard tool

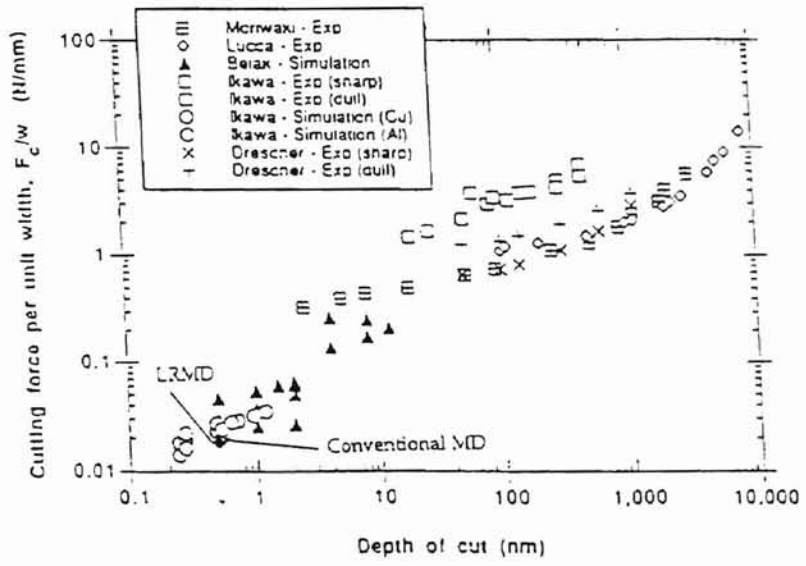

Fig. 5.9 Variation of the cutting force per unit width versus the depth of cut (both experimental and simulation data) obtained from the literature. Also shown are the data obtained for a cutting depth of 0.724 nm by Conventional MD and LRMD methods

Figures 5.10 and 5.11 show the variation of computational time and required memory space, respectively, versus the cutting distance. It can be seen that as the cutting distance increases the difference in the computational time between the conventional method and LRMD becomes significant. The advantage of using LRMD in terms of significant reduction (atleast 2 times) in the computational time and required memory space can clearly be seen. After a specified length of cut, the number of atoms in the workmaterial can be maintained more or less constant using the LRMD technique (Table 5.4). As a result, the memory space can also be maintained more or less constant irrespective of the cutting length (Table 5.4).

The final step is to check the validity of using LRMD for nanometric cutting. The force plots shown in Figure 5.12 and Figure 5.13 correspond to the cutting force and thrust force data obtained by cutting the workmaterial for a distance of 100 Å using the conventional and LRMD methods. The average cutting forces by the conventional MD and LRMD methods are 33.25 eV/Å (3.678×10^{-2} N/mm) and 33.865 eV/Å (3.746×10^{-2} N/mm), respectively. Similarly, the average thrust force by the conventional MD and LRMD methods are 24.551 eV/Å (2.716×10^{-2} N/mm) and 24.552 eV/Å (2.716×10^{-2} N/mm), respectively. It can thus be seen that the results obtained by both methods are in general agreement.

The variation in the force values, which are small and negligible, are attributed to the differences in the total number of atoms considered. Also, this difference in the force curve is due to the random velocity assigned to the atoms added to the leading edge, which is not the same as the atom velocities of a larger workmaterial. However, this difference is of small magnitude as can be seen from the average force values (cutting and thrust force) obtained by both methods and hence can be neglected.

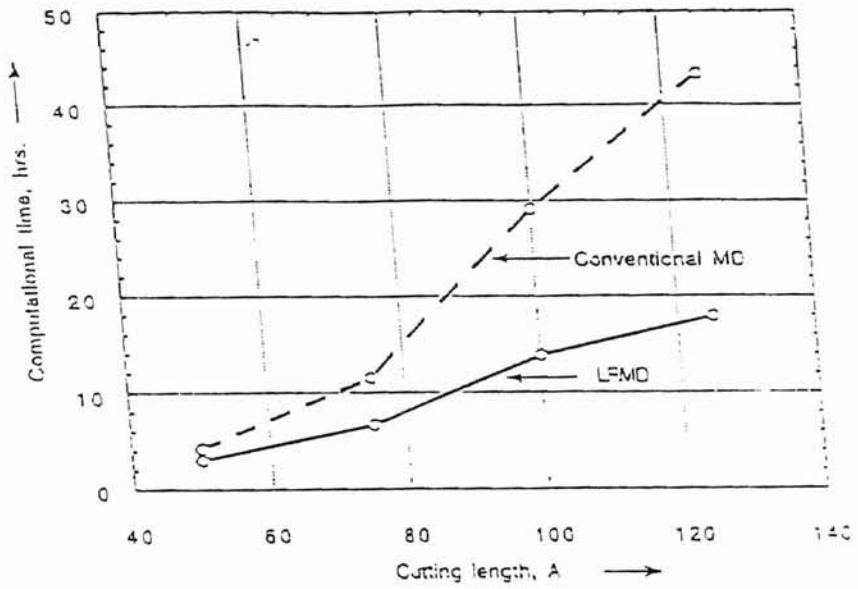

Fig. 5.10 Variation of computational time versus cutting distance by Conventional MD and LRMD methods

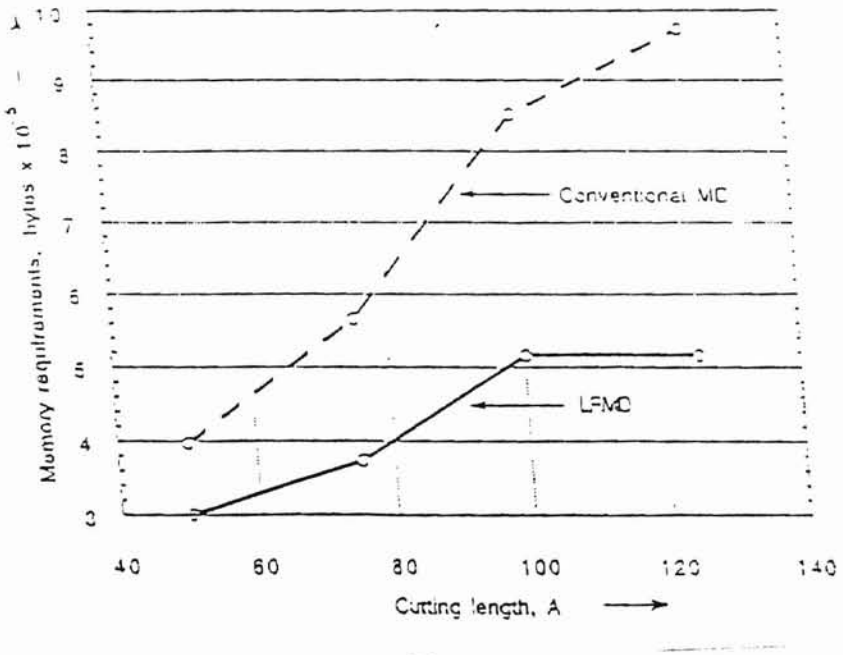

Fig. 5.11 Variation of required memory space versus cutting distance by Conventional MD and LRMD methods

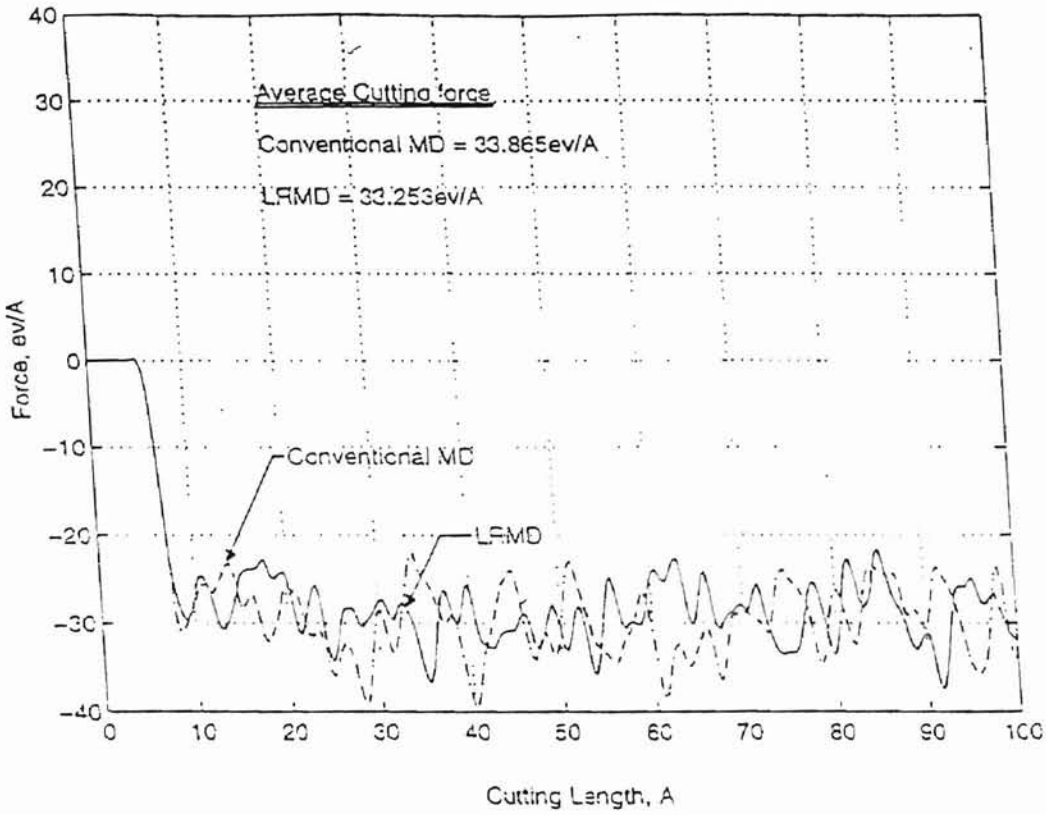

Fig. 5.12 Cutting force data obtained by cutting the workmaterial for a distance of 100 angstroms using Conventional MD and LRMD methods

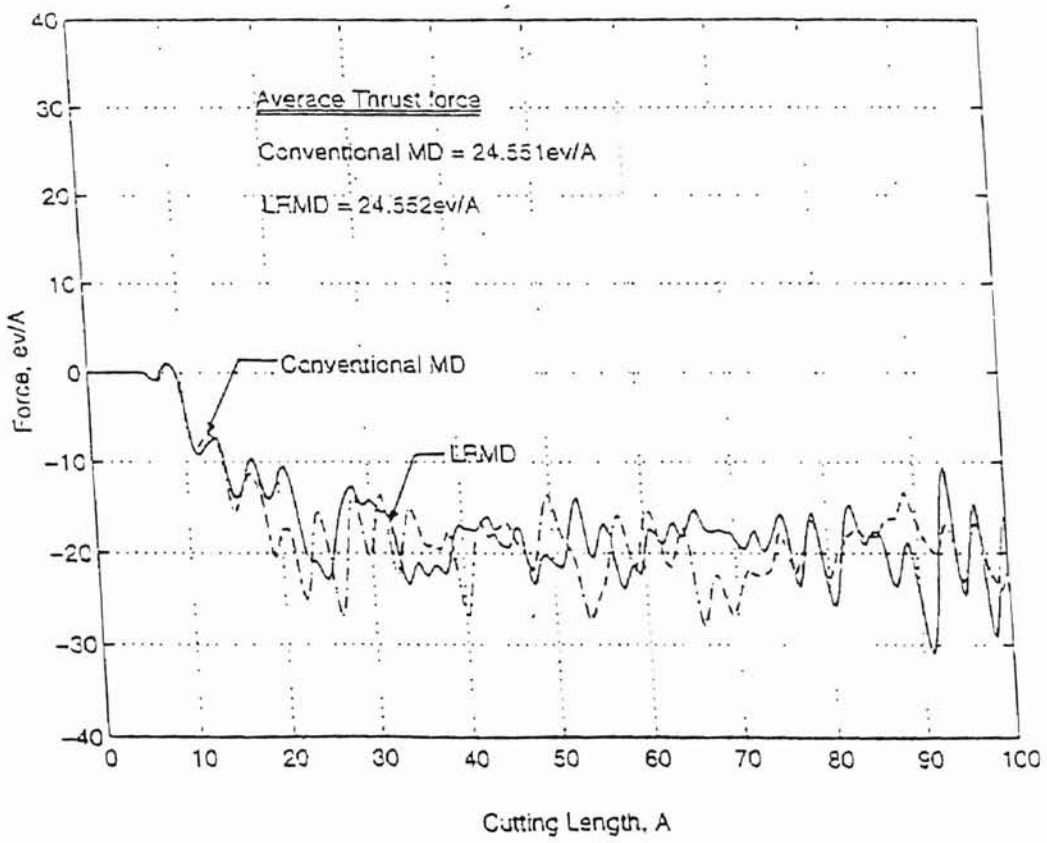

Fig. 5.13 Thrust force data obtained by cutting the workmaterial for a distance of 100 angstroms using Conventional MD and LRMD methods

Good agreement between the force values was also obtained for different workmaterial sizes, cutting distances, depths of cut, and cutting speeds for the conventional and LRMD thus confirming the validity of LRMD over a wide range of cutting conditions. It may be noted that the scope of this investigation is much broader than nanometric cutting as the principle can be applied for any MD simulation.

5.5. Advantages

By implementing Length Restricted Molecular Dynamics (LRMD) simulation approach the following advantages can be realized.

1. Significant reduction in the computational time (atleast 2-3 times), depends on the number of atoms considered.
2. Reduced computer memory requirements (atleast 2-3 times) which also depends on the number of atoms considered.
3. By implementing LRMD it is possible to reduce the cutting speed used in the simulations by a factor of 2 or 3.

However, to enable use of cutting speeds that are used in practice, further advancements in the computational speed is necessary and it may be a long way before practical cutting speeds can be used in MD simulations and obtain the results in a reasonable computational time frame.

CHAPTER 6

LRMD SIMULATION TO STUDY MACHINING WITH NEGATIVE RAKE TOOLS SIMULATING GRINDING

6.1. INTRODUCTION

Grinding is technologically an important manufacturing operation for finishing. It is estimated that about 20% of all the manufacturing operations are by grinding. Current ultraprecision grinding machines use diamond/CBN abrasives at chip sizes on the order of a few nanometers. However, unlike the multipoint tools such as milling cutters, the geometry of the abrasives in grinding is not fixed and their geometry changes continuously as the process proceeds. However, it is widely known that the abrasive grits in grinding present a large negative rake angle. This is based on the ratio of the forces, energy expended in grinding, and subsurface deformation in grinding compared to conventional machining.

In order to understand the material removal mechanisms in grinding, it becomes necessary to conduct experiments with high negative rakes. There is a need to know whether with high negative rake tools material is removed by chip formation or by ploughing of the tool into the workmaterial. Rubenstein et al. (1966) concluded that no chips will be formed when cutting with tool rake angles more negative than -55 degrees. However, this result as Komanduri (1971) pointed out was based on extrapolation of results published by Crawford and Merchant (1953) for tools with zero rake angle to 55 degrees rake angle.

To simulate grinding, Komanduri (1971) conducted single point cutting with a wide range of negative rake angle tools (up to -85°). In this work, he found that the formation of chips not only depends on the rake angle but also depends on the width of the workmaterial being machined for a given depth of cut. Reduction in the width of the workmaterial minimizes the possibility of plane strain conditions. This results in poor friction conditions on the rake face. In such a case material removal is through ploughing and side spread of the workmaterial. He also observed the absence of chip formation with a -85 degree rake tool and not -55 degree rake as postulated by Rubenstein et al. (1966). The tool merely rubbed the worksurface resulting in plastic deformation and side flow. With a 10 degree rake Komanduri (1971) reported the thrust force to be 0.9 times the cutting force. As the rake angle was decreased to more negative values, the thrust force was observed to increase initially slowly, up to about -50 degrees and then a sharp rise up to -85 degrees. However, the depth of cut was of necessity limited to 10 μm in that investigation as it was conducted on a conventional lathe and not a ultraprecision lathe capable of nanometric cutting. In the present investigation, in order to obtain a better understanding of the material

removal mechanisms in UPG at nanometric level, MD simulation was conducted with an uncut chip thickness of 0.724 nm and various negative rake angles (-75° to +45°). Cutting forces, specific energy, subsurface deformation, and size effect are studied by comparing with the experimental results of Komanduri (1971).

6.2. MD SIMULATION CONDITIONS

Table 6.1 lists the MD simulation conditions used for different tool rake angles.

Table 6.1 MD Simulation Conditions for Various Rake Angles

S.No.	Length of cut (Å)	Workmaterial dimensions (units)	Tool dimensions (units)	Depth of cut (Å)	Rake angle (in degrees)	Clearance angle (in degrees)
1	75.0	4x21x20	4x10x14	7.24	-75	5
2	75.0	4x21x20	4x10x14	7.24	-60	5
3	75.0	4x21x20	4x10x14	7.24	-45	5
4	75.0	4x21x20	4x10x14	7.24	-30	5
5	75.0	4x21x20	4x10x14	7.24	-15	5
6	75.0	4x21x20	4x10x14	7.24	-5	5
7	75.0	4x16x20	4x10x14	7.24	0	5
8	75.0	4x16x20	4x10x14	7.24	5	5
9	75.0	4x16x20	4x10x14	7.24	10	5
10	75.0	4x16x20	4x10x14	7.24	15	5
11	75.0	4x21x20	4x10x14	7.24	30	5
12	75.0	4x21x20	4x10x14	7.24	45	5

As previously stated, the MD simulations were conducted on a Digital alpha workstation with a clock speed of 333MHz. Pairwise Morse potential was used to model the copper workmaterial. An infinitely hard tool (tungsten) was used in the MD simulation of nanometric cutting at a cutting speed of 500m/s. The computational parameters listed in Table 5.3 (Chapter 5) were used in this investigation as well.

6.3. RESULTS AND DISCUSSION

Table 6.2 gives the mean cutting force, thrust force, ratio of the thrust force to the cutting force, and the specific energy for the MD simulation of nanometric cutting with tools of different rake angles.

Figure 6.1 is the variation of the cutting and the thrust forces with rake angle. It can be seen that as the rake angle is changed to more negative, thrust force increases gradually, up to -30° and then shows a sharp rise at -45° up to -75°. The cutting force also shows a similar trend but at a slower rate. These trends are similar to the results reported by Komanduri (1971). Figure 6.2 shows the variation of the ratio of the thrust force to the cutting force with the rake angle and this ratio increases as the rake changes to more negative. At 15 degree rake the thrust force is 0.6 times the cutting force. This ratio increases as the rake changes to more negative. It can be seen from Table 6.2 that the thrust force is 1.9 times (~ 2 times) the cutting force at -60°. Marshall and Shaw (1952) found the mean grinding coefficient, which is the ratio of cutting force to thrust force for grinding to be 0.47 for silicon carbide wheel. In this simulation study, the thrust force is ~ 2 times the cutting force at -60° suggesting a similarity between the UPG and the nanometric cutting with high negative rake tools.

Table 6.2 Results of MD Simulation of Nanometric Cutting with Various Rake Angles Simulating Grinding

S.No	Rake Angle, degrees	Width of cut (Å)	Cutting force per unit width x 10^{-2}, N/mm	Thrust force per unit width x 10^{-2}, N/mm	Thrust force/ Cutting force	Specific energy x 10^5, mmN/mm^3
1	45	14.48	2.124	1.054	0.496	0.293
2	30	14.48	2.238	1.276	0.57	0.309
3	15	14.48	2.661	1.582	0.5945	0.368
4	10	14.48	2.921	1.939	0.6638	0.403
5	5	14.48	3.33	2.472	0.7423	0.46
6	0	14.48	3.631	3.116	0.8581	0.502
7	-5	14.48	3.813	3.687	0.9669	0.527
8	-15	14.48	4.506	4.887	1.085	0.622
9	-30	14.48	4.938	6.92	1.4014	0.682
10	-45	14.48	6.132	10.6	1.7286	0.847
11	-60	14.48	6.485	12.336	1.9022	0.896
12	-75	14.48	7.321	17.286	2.361	1.011

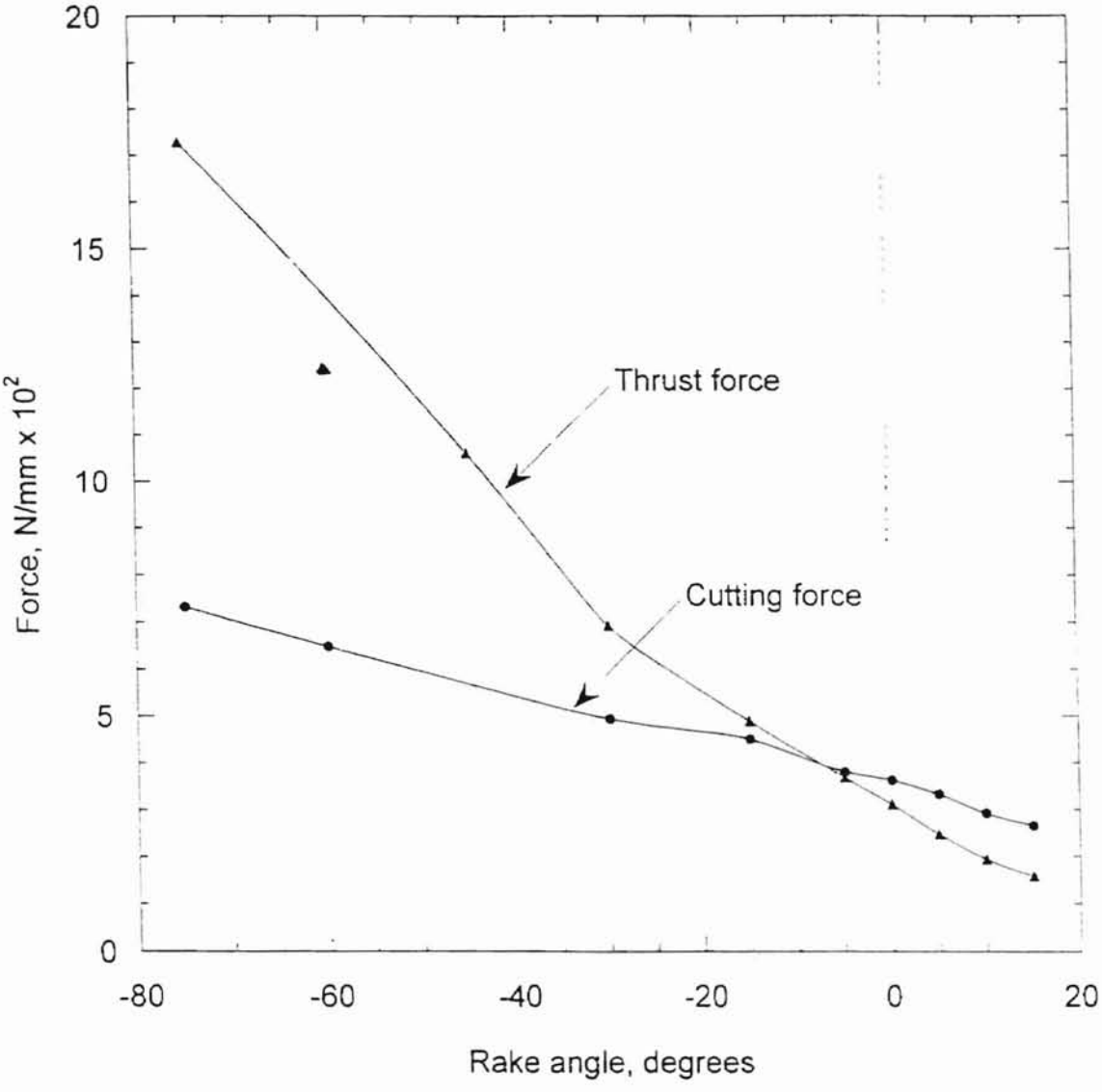

Fig. 6.1 Variation of cutting and thrust forces with rake angle in nanometric cutting

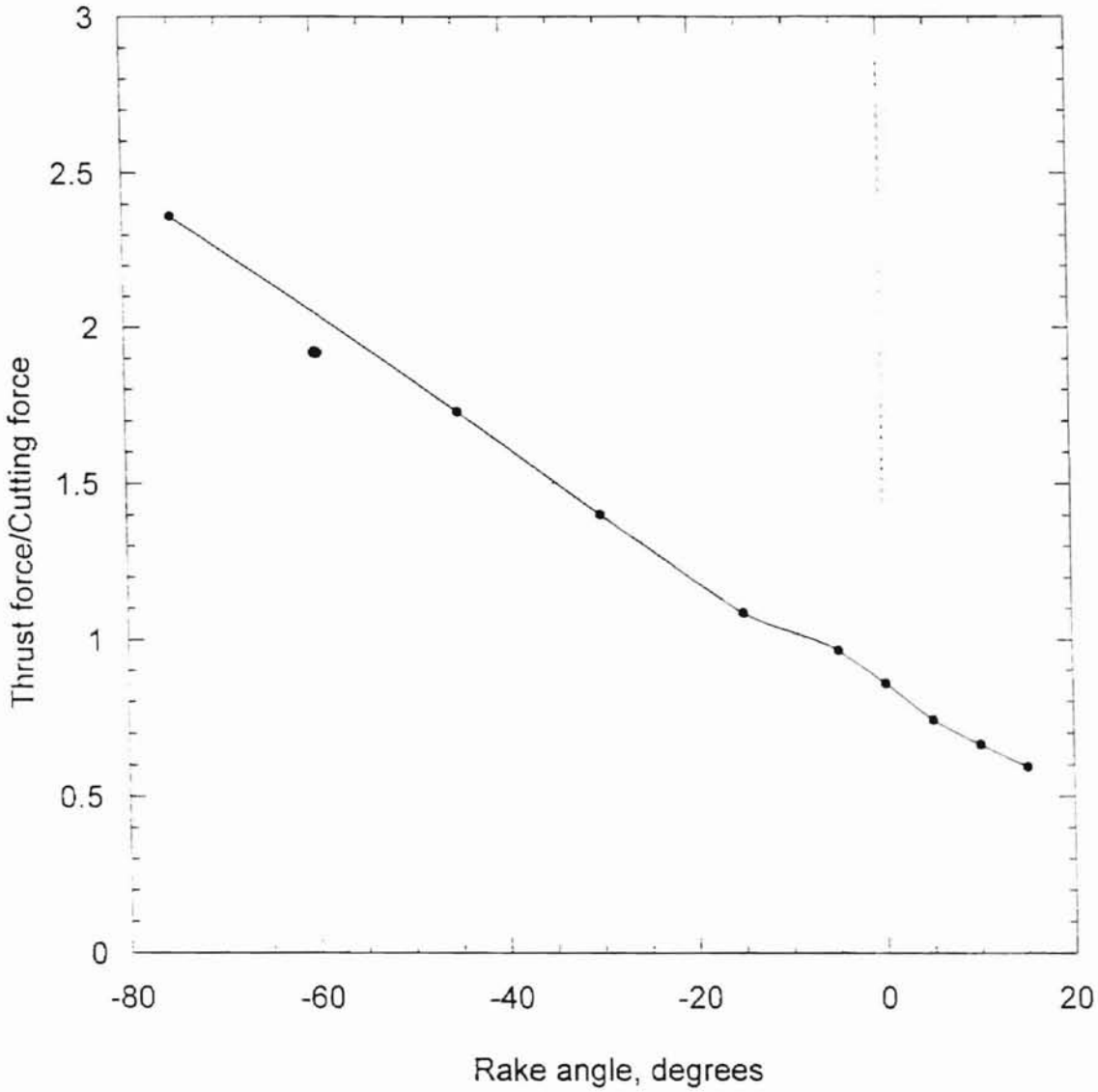

Fig. 6.2 Variation of force ratio against rake angle in nanometric cutting

The trends shown in Figures 6.1 and 6.2 are in agreement with the plot shown in Figure 6.3 (Komanduri 1971) from literature.

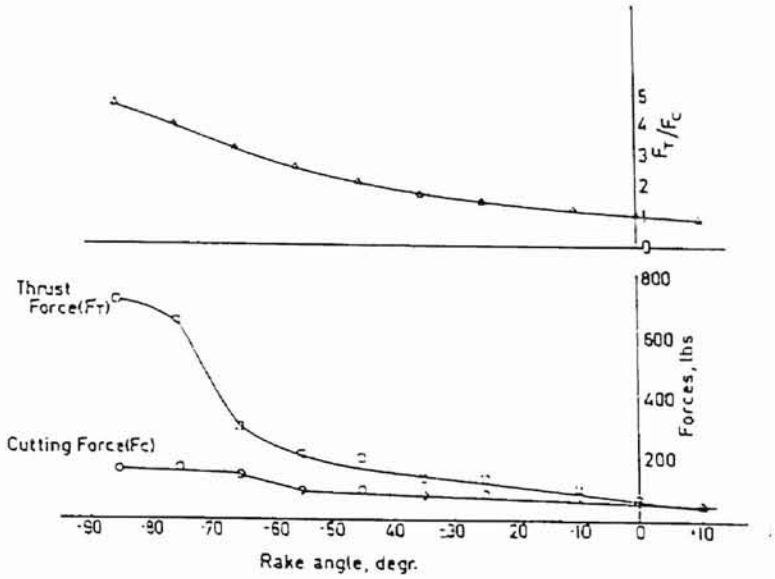

Fig 6.3 Variation of forces and force ratio with rake angle (Komanduri 1971)

From Figure 6.4 it can be seen that for negative rake the chip has to be more deformed, requiring more work to be done on it and hence more pressure on the tool face. This reason alone might cause both the cutting force and the thrust force to increase about the same amount. But, beyond this, consider the inclination of the tool face as shown in Fig. 6.5. The main force on this face will be the pressure of the chip pushing perpendicular to it. A lesser force will be the friction force acting parallel to this face as the chip tries to pull the tool face upward, along with it.

For the positive rake tool, the main force is slightly downward, cancelling out some of the upward force due to friction, in fact, with high positive rakes it is possible to get these forces just balanced so that there is practically very little or no thrust force. It is also possible to get the downward force to dominate so that the forces are actually pulling the tool into the work, rather than pushing it away.

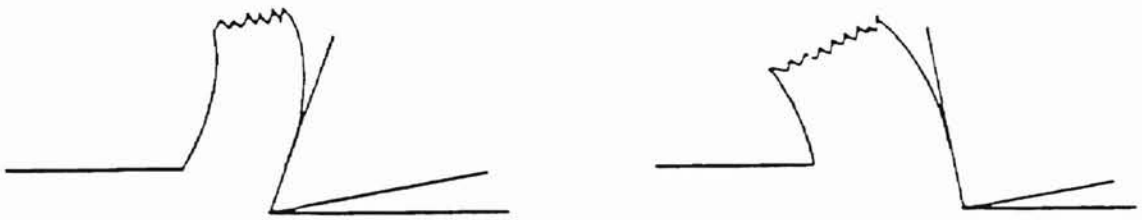

Fig. 6.4 Illustration of chip formation while cutting with positive and negative rake tools

Fig. 6.5 Effect of tool face inclination on cutting force and thrust force

On the other hand, with a negative rake, since the rake face is aimed downward, both components of force are acting in the upward direction, therefore, one can expect the net force to be a strong upward push. This

reasoning tells us that the cutting force (F_c) should go up as rake becomes more negative, but that the thrust force (F_t) should increase by a much greater percentage.

An increase in specific energy was observed with decrease in the rake angle. Figure 6.6 is the graph between the specific energy and the tool rake angle in comparison to the experimental results by Komanduri (1971).

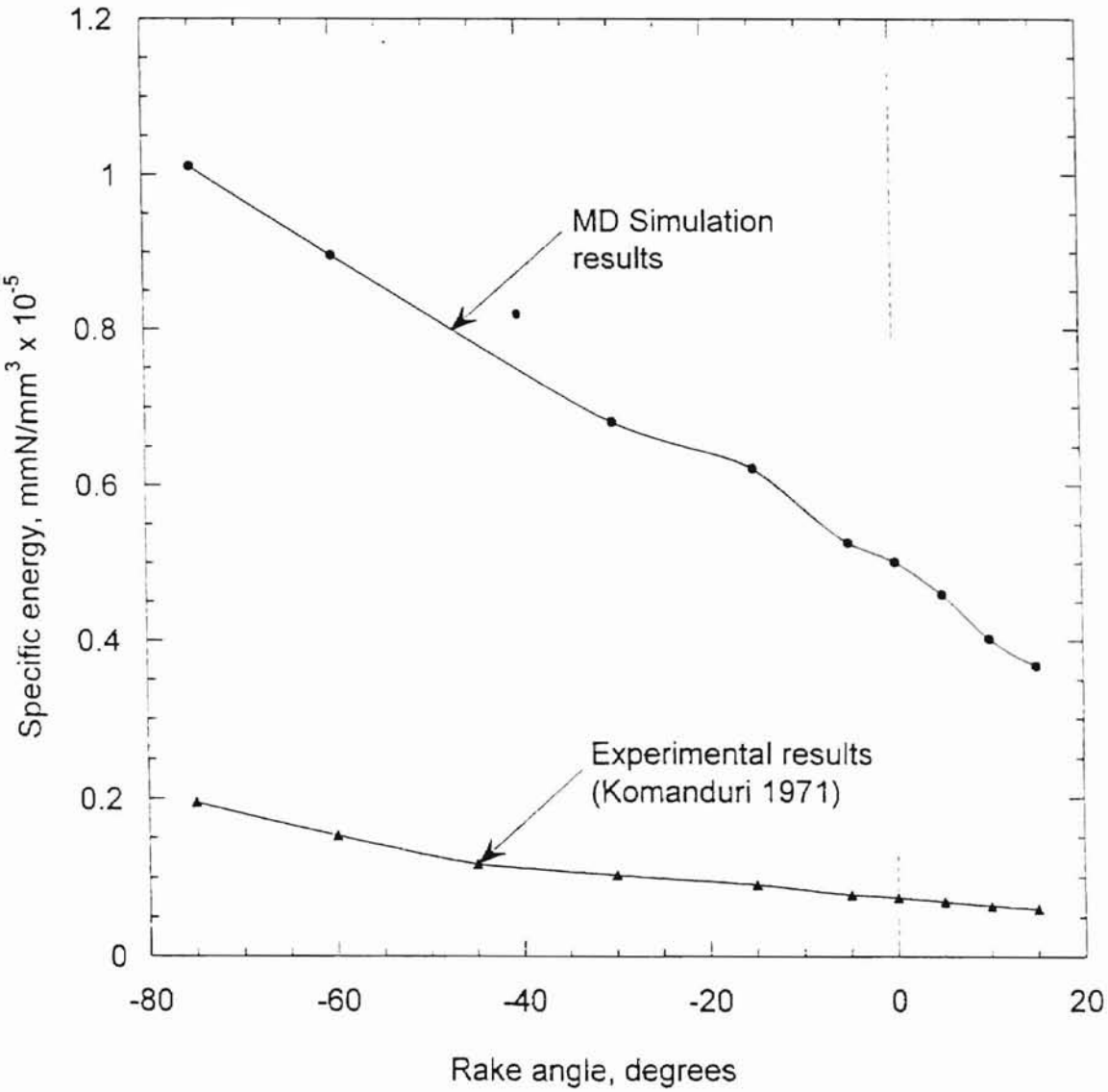

Fig. 6.6 Variation of specific energy with rake angle in nanometric cutting obtained for a cutting depth of 0.724 nm. Also shown are the experimental data (Komanduri 1971) obtained for a cutting depth of 10 μm.

It can be inferred from Figure 6.6 that the specific energy in nanometric cutting is an order of magnitude larger (~6 to 7 times) than conventional cutting. Since, this increase in specific energy is not proportional to the decrease in depth of cut and consequently, it can be attributed to the size effect reported by researchers (Furukawa et al. 1988, Moriwaki et al. 1989, Lucca et al. 1991). Figure 6.7 is the specific energy curve plotted using the experimental values by Komanduri (1971). The trend of Fig. 6.6 is in agreement with the experimental curve as in Fig. 6.7. The sudden increase in the cutting force from -30° to -45° (Fig. 6.1) is reflected by a corresponding increase in the specific energy.

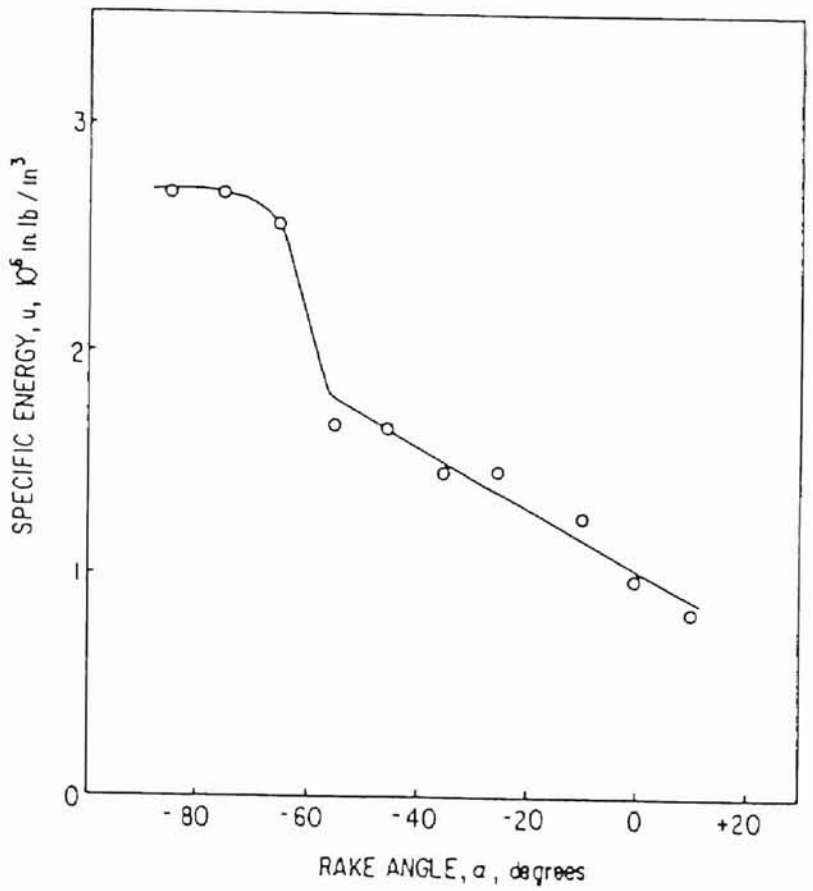

Fig. 6.7 Specific energy in orthogonal machining versus rake angle (after Komanduri 1971)

Figures 6.8 (a)-(g) are the photographs of the nanometric cutting process conducted with various rake tools. Plastic deformation ahead of the tool tip and into the machined surface can be clearly seen. The chip length reduces with decreasing rake angle with length, width, and depth of cut maintained constant. Since, the volume of material removed is constant, the reduction in chip length suggests side flow of the workmaterial. Figures 6.8 (a) - (g) also suggests increased plowing of the tool into the workmaterial with increased negative rake tools.

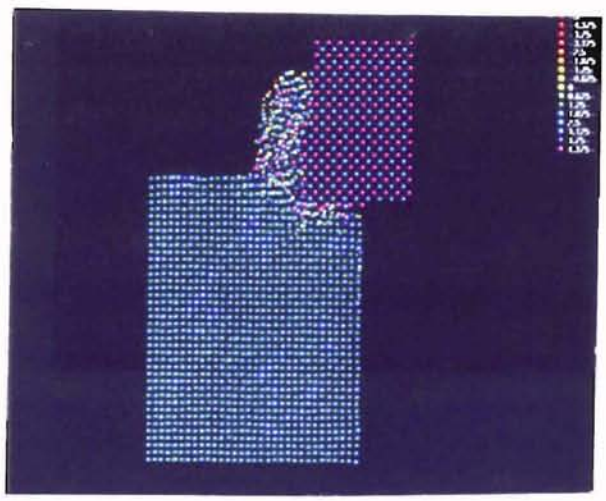

Fig. 6.8 (a) Photograph of the nanometric cutting process with 5 degree rake tool

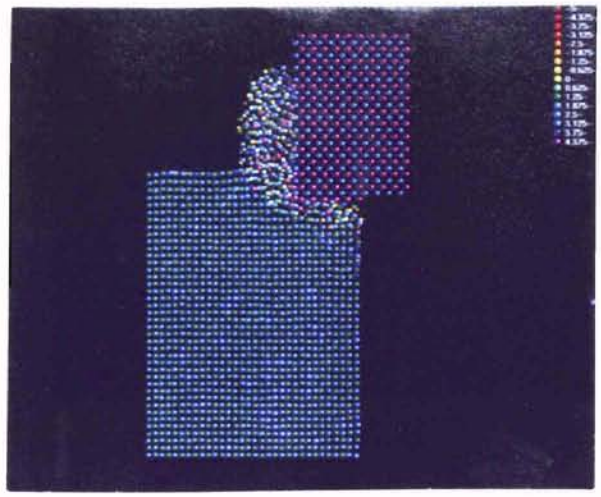

Fig. 6.8 (b) Photograph of the nanometric cutting process with 0 degree rake tool

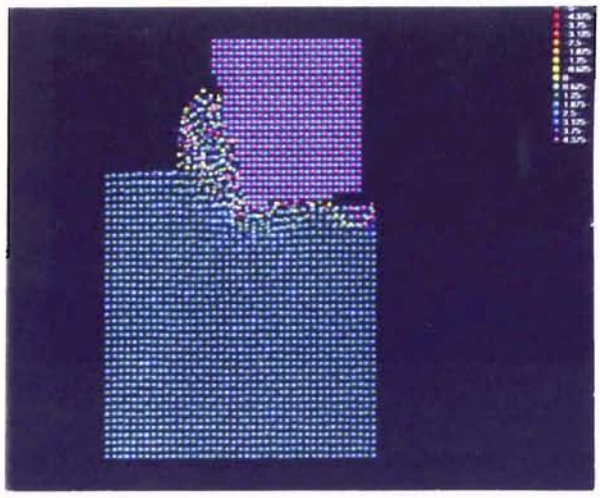

Fig. 6.8 (c) Photograph of the nanometric cutting process with -15 degree rake tool

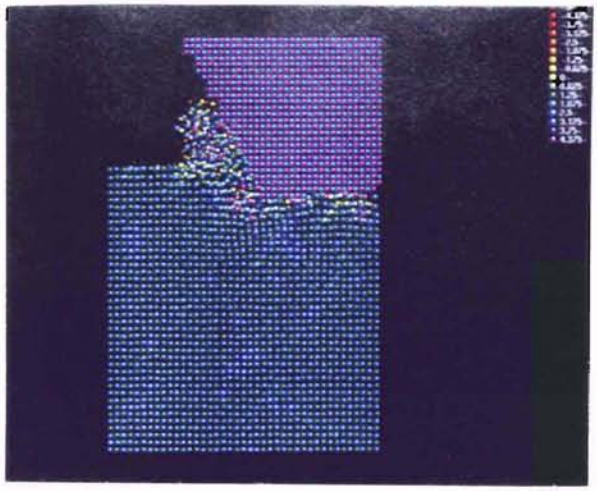

Fig. 6.8 (d) Photograph of the nanometric cutting process with -30 degree rake tool

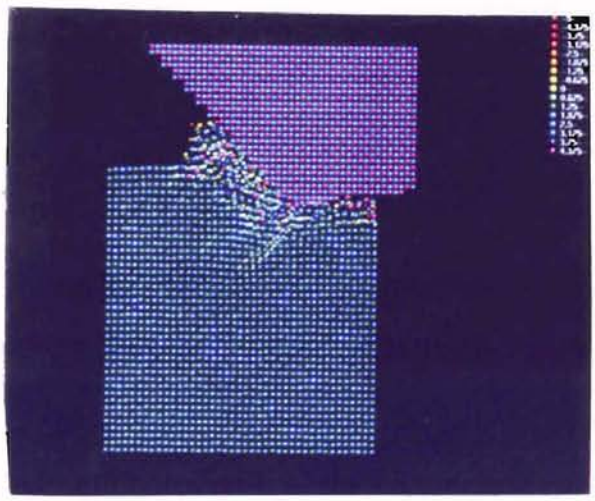

Fig. 6.8 (e) Photograph of the nanometric cutting process with -45 degree rake tool

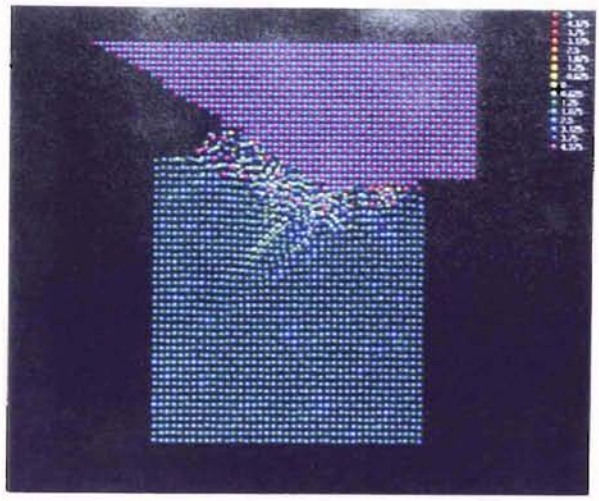

Fig. 6.8 (f) Photograph of the nanometric cutting process with -60 degree rake tool

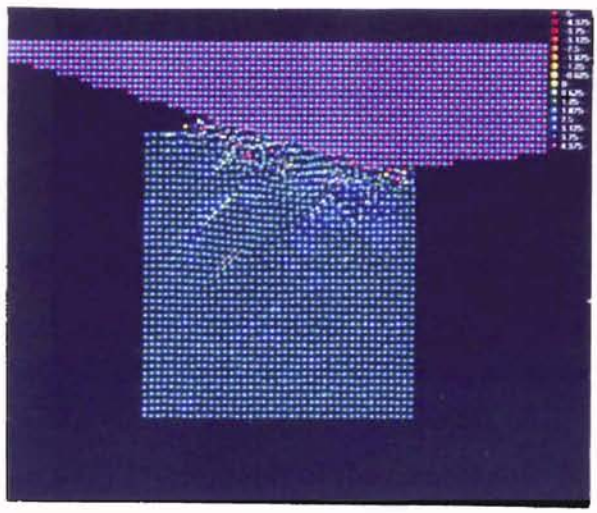

Fig. 6.8 (g) Photograph of the nanometric cutting process with -75 degree rake tool

Comparison of Figures 6.8 (a)-(g) and computer animated movies of the nanometric cutting process also suggests an increase in the degree of subsurface deformation with decrease in rake angle. The computer animated movies also show the generation and movement of dislocations in the workmaterial. Once the tool has passed the machined zone, recession of dislocations due to elastic recovery of the workmaterial was also observed. Chip curl was observed for high positive rake tools (+30 and +45 degrees). As the rake drops down to more negative values the shear plane rotates towards the workmaterial. This rotation of the shear plane can be attributed to decrease in shear angle with increase in the negative rake.

CHAPTER 7

CONCLUSIONS

Ultraprecision machining is currently being used to produce optical, mechanical, and electronic components which require submicrometer form accuracies and nanometer scale surface roughness. This technology has been successfully used to extend the limits of geometric accuracy and surface finish of parts to nanometric level. The regime in which the technology is successfully applied can be extended by a better understanding of the material removal process at nanometric level. However, our understanding of material removal mechanisms at such small depths of cut is somewhat limited by technological difficulties in measuring forces and observing chip formation process. Since, the material removed in UPM is on the order of a few Å, MD simulation can be used as an alternate approach to study UPM/UPG at nanometric level. However, MD simulation of nanometric cutting involves considerable computational time (a few days to several weeks) and significant computer memory usage even for a few thousand workmaterial atoms. Consequently, it becomes necessary to use one of the

following alternatives: extremely high cutting speed (~500 m/sec.), simulations using fewer number of atoms, 2-D modelling, or accept long computational times to address such problems. In order to implement 3-D cutting even at very high cutting speeds the processing times have to be reduced. This can be facilitated by increasing the processing speed using faster computers or by developing simulation techniques that can reduce both the computational time and memory space requirements.

In this investigation, Molecular Dynamics (MD) simulation of nanometric cutting was used to study ultraprecision machining. It involved the development of a new method for reducing the computational time and required computer memory space for conducting MD simulations (LRMD method). This technique was extended to study machining with large negative rake tools simulating grinding. This chapter summarizes the conclusions of this investigation.

7.1. LENGTH RESTRICTED MOLECULAR DYNAMICS

A new technique termed Length Restricted Molecular Dynamics (LRMD) simulation of nanometric cutting was developed to reduce the computational time and memory space requirements. A code in C programming language was developed to implement this method in the current conventional MD simulation technique. A significant reduction in the computational time and required memory space (~ 2 to 3 times) which becomes more significant as the number of atoms considered increases was achieved by implementing LRMD. For example, from Table 5.4 (Chapter 5), for a cutting length of 100 Å by conventional MD the computational time and memory used were 29:10:16 hrs. and 851827 bytes whereas, by LRMD these

values were reduced to 13:49:30 hrs. and 516703 bytes. When LRMD is applied reduced cutting speeds (~ 2 to 3 times) can be used and yet obtain results in a reasonable computational time frame. Using this method, practically any length of workmaterial can be cut with a constant length of the workmaterial during simulation. LRMD simulation technique was verified by comparing the results with conventional MD simulation results. The average cutting forces by the conventional MD method and LRMD technique were 33.25 eV/Å (3.678×10^{-2} N/mm) and 33.865 eV/Å (3.746×10^{-2} N/mm), respectively. Similarly, the average thrust force by the conventional MD and LRMD methods were 24.551 eV/Å (2.716×10^{-2} N/mm) and 24.552 eV/Å (2.716×10^{-2} N/mm), respectively. It can thus be seen that the results obtained by both methods are in general agreement. The ratio of cutting force to thrust force by LRMD method was 1.3543 which is on the same order of magnitude as in conventional machining. The simulation results were also compared and found to be in reasonable agreement with the experimental and simulation results reported in the literature.

7.2. MD SIMULATION OF NANOMETRIC CUTTING WITH HIGH NEGATIVE RAKE ANGLE TOOLS SIMULATING GRINDING

Grinding is technologically an important manufacturing operation. In UPG, a multipoint grinding wheel is used to remove material at chip sizes on the order of a few nanometers. However, unlike multipoint tools (e.g. milling cutters), the geometry of the abrasive grits in UPG are not fixed and their geometry changes continuously as the process proceeds. This increases the complexity in understanding the material removal mechanisms in

grinding. Komanduri (1971) conducted single point cutting with large negative rake angle tools (up to -85°) to simulate grinding. However, the depth of cut in that work was limited to 10 μm by necessity, as a conventional lathe was used. In order to facilitate a better understanding of the material removal mechanisms at nanometric level in UPG, MD simulations were conducted with various negative rake tools (+45 to -75 degrees) to simulate grinding. LRMD technique was employed in this investigation to extend its application and to reduce the computational time and memory space. The two components of the cutting force, specific energy, subsurface deformation, and size effect were studied by comparing the simulation results with experimental results of Komanduri (1971). An increase in specific energy (0.3675×10^5 mmN/mm^3 at 15° rake to 0.895×10^5 mmN/mm^3 at -60° rake), cutting and thrust forces, and ratio of thrust force to cutting force (0.5943 at 15° rake to 1.902 at -60° rake) was observed with increase in the negative rake angle. The increase in specific energy in nanometric cutting was found to be an order of magnitude larger than conventional cutting (6 to 7 times). This increase is attributed to the decrease in depth of cut and hence the size effect. Also, the degree of subsurface deformation was found to increase with decrease in rake angle. As the rake angle decreases to more negative values a transition in the process from cutting dominant to plowing/indentation dominant process was observed. The length of the chip was observed to decrease with increasing negative rake tools for a constant length and depth of cut. The shear plane was observed to rotate towards the workmaterial with a drop in the rake angle which corresponds to a decrease in the shear angle with increasing negative rake. The results observed and reported in this investigation are in agreement with the results reported by other researchers

(Komanduri 1971, Furukawa et al. 1988, Moriwaki et al. 1989, Lucca et al. 1991).

7.3. FUTURE WORK

MD simulation is usually conducted on a perfect crystal with the assumption that there are no defects in the system. However, real crystals deviate from the perfect periodicity assumed in most of the simulation work. While this concept of perfect system is adequate for explaining the structure-insensitive properties of metals, it is necessary to consider various types of lattice defects for a better understanding of structure-sensitive properties Dieter 1986).

A system is said to be a defective system if there is any deviation from the periodic arrangement of the lattice. When this defect is localized to the vicinity of a few atoms, the defects are known as point defects. However, if the defect extends through microscopic regions of the crystal, it is called a lattice imperfection which may be divided into line defects and plane defects. Line defects propagate as a 2-dimensional network in the crystal. Edge and Screw dislocations are examples of line defects. When line defects cluster into a plane, plane defects arise. Stacking fault between two close packed regions of the crystal that have alternate stacking sequences and twinned region of a crystal are examples of plane defects.

In our MD simulation attempts are on to investigate the role of point defects and line defects in a system. A code in C was written to introduce point defects (Vacancies, interstitials, and impurities) and edge dislocations into the workmaterial. The impurities introduced are considered as infinitely hard and their motion is not tracked. Currently work is being carried out to

extend the new MD simulation technique to understand the effects of the lattice defects at atomic level. Some of the future work suggested in this field are,

1. To study the effect of density of vacancies in a crystal lattice and hence to study the formation of voids

2. To study the effects of impurities in the workmaterial and the local disturbances caused by these impurities to the periodicity of the lattice

3. To observe the movement of dislocations through the crystal lattice and to identify Burger's vector

4. To study the effect of dislocations with different orientations

The new MD simulation technique can also be extended to ultraprecision diamond turning of aluminum and copper workmaterials in different crystallographic orientations using a single crystal diamond tool to facilitate study on the effect of crystallographic anisotropy on the cutting behavior, mechanism of chip formation, and cutting force.

REFERENCES

Agrawal, M. P., Raff, L. M., and Thompson, D. L., 1987, Surf. Sci. 188, 402.

Alder, B., and Wainwright, T., 1959, J of Chemical Physics, 31, No. 2, 459.

Alder, B., and Wainwright, T., 1960, J of Chemical Physics, 33, No. 5, 1439.

Allen, M., and Tildesley, D., 1991, "Computer Simulation of Liquids," Oxford University Press, Oxford, U. K.

Belak, J., and I. F. Stowers, 1990, Proc. ASPE Annnual Conf., Rochester, NY, 76.

Belak, J., Lucca, D. A., Komanduri, R., Rhorer, R. L., Moriwaki, T.,Okuda, K., Ikawa, Shimada, S., Tanaka, H., Dow., T. A., Drescher, J. D., and I. F. Stowers, 1991, Proc. of the ASPE Annual Conference, 100.

Belak, J., 1994, Energy & Technology Review , Lawrence Livermore Laboratory, 13.

Belak, J and I. F. Stowers, 1995, Private Communication

Brenner, D. W., Sinnott, S. B., Harrison, J. A., and Shenderova, O. A., 1996, Nanotechnology, 7, 161.

Brown, N. J., Donaldson, R. R., and Thompson, D. C., 1983, The Int. Soc. Opt. Eng., Vol. 381, 48.

Bryan, J. B., 1979, Precision Engineering, 1, No.1, 13

Chang, X, Perry, M., Peploski, J., Thompson, D, and Raff, L., 1993, J. Chem. Phys. , 99, 4748

Chang, X., Thompson, D., and Raff, L., 1993, J. Chem. Phys. , 97, 10112.

Chang, X., Thompson, D., and Raff, L., 1994, J. Chem. Phys., 100, 1765.

Crawford, J. H., and Merchant, M. E., 1953, Trans. Am. Soc. Mech. Engrs., 75, 561.

Dodson, B. W., 1990, Solid State and Materials Sciences, 16, No. 2, 115.

Donaldson, R. R., 1983, SPIE, Vol. 433, 62.

Feynman, R. P., "Miniaturization by D. H. Gilbert", Newyork, NY, 1961.

Franks, A., 1988, ASPE 3rd Annual Precision Engineering Conf., Atlanta, 20.

Furukawa, Y., and Moronuki, N., 1988, Annals of CIRP, 37, 1.

Goldstein, H., 1965,"Classical Mechanics," Addison-Wesley Reading, MA.

Goodfellow, J. M., 1990, "Molecular Dynamics: Applications to Molecular Biology," CRC Press Inc.

Haile, J., 1992, " Molecular Dynamics Simulation Elementary Methods, "John Wiley & Sons, Inc.

Hoover, W. G., 1986,"Molecular Dynamics," Lecture Notes in Physics, 258 Springer-Verlag, Berlin, 13

Hoover, W. G., Hoover, C. G., and I. F. Stowers, 1989, Fabrication Technology, Mat. Res. Symposium, 140, 119.

Hoover, W. G., De Groot, A. J., Hoover, C. G., Stowers, I. F., Kawai, T., Holian, B. L., Boku, T., Ihara, S., and Belak, J., 1990, Physical Review A, 42, No. 10, 5844.

Ikawa, N., Shimada, S., Tanaka, H., 1990, 2nd Nanotechnology Seminar, University of Warwick, Coventry, U. K.

Ikawa, N., Shimada, S., Tanaka, H., and Ohmori, G., 1991, Annals of the CIRP, 40/1, 551.

Ikawa, N., 1995, Private Communication.

Inamura, T., Suzuki, H., and Takezawa, N., 1991, Int. J. Japan Soc. Prec. Eng., 25, No. 4, 259.

Inamura, T., Takezawa, N., and Taniguchi, N., 1992, Annals of the CIRP, 41/1, 121.

Inamura, T., Takezawa, N., and Kumaki, Y., 1993, Annals of the CIRP, 42/1, 79.

Inamura, T., Takezawa, N., Kumaki, Y., and Sata, T., 1994, Annals of the CIRP, 43/1, 47.

Kim. D.E. and Suh, N. P., 1994, Trans ASME, J of Tribology, 116, 225.

Komanduri, R., 1971, Int. J. Mach. Tool Des., Vol. 11, 223.

Landman, U., Luedtke, W., Burnham, N., and Colton, R., 1990, Science, 248/17, 454.

Levine, R., and Bernstein, R., 1987, Molecular Reaction Dynamics and Chemical Reactivity," Oxford University Press, Oxford, U.K.

Lucca, D. A., Rhorer, R. L., Komanduri, R., 1991, Annals of CIRP, Vol. 40/1, 69.

Lucca, D. A., Seo, Y. W., 1993, Annals of CIRP, Vol. 42/1, 83.

Lucca, D. A., Seo, Y. W., 1994, Tribology Transactions, 37/3, 651.

Maekawa, K., and Itoh, A., 1995, Wear, 188, 15.

Marshall, E. R., and Shaw, M. C., 1952, Trans. Am. Soc. Mech. Engrs., 74, 51.

McKeown, P. A., 1982, SME Technical Paper, MR 82.

McKeown, P. A., 1987, Annals of CIRP, 36/2, 495.

McKeown, P. A., 1996, Sensor Review, Vol. 16, No. 2, 4.

Moriwaki, T., and Okuda, K., 1989, Annals of CIRP, Vol. 38/1, 115.

Nakayama, K., and Tamura, K., 1968, Trans. ASME J. Eng. Ind., 119.

Peploski, J., Thompson, D. and Raff, L., 1992, J. Chem. Phys., 96, 8538.

Perry, M., and Raff, L., 1994, J. Phys. Chem., 98 4375.

Perry, M., and Raff, L., 1994, J. Phys. Chem., 98, 8128.

Raff, L., 1992, J. Chem. Phys. 97, 7459.

Raff, L.M. and Thompson, D. A.,"The Classical Trajectory Approach to Reactive Scattering," Chapter 1, Volume 3 inTheory of Chemical Reaction Dynamics, Ed. Michael Baer, CRC Press, (1986) 2-121

Rentsch, R. and Inasaki, I., 1994, Annals of CIRP 43/1, 327.

Riley, M. E., Coltrin, M. E., and Diestler, D. J., 1988, J. of Chemical Physics, 88, 5943.

Rubenstein, C., Groszmann, F. K., and Koenigsberger, 1966, Proc. Int. Industrial Diamond Conf., Oxford, Vol. 1, 161. Industrial Diamond Information Bureau, London (1967).

Seo, Y., 1993, Doctoral Thesis Report, Oklahoma State University.

Shimada, S., Ikawa, N., Ohmori, G., and Tanaka, H., 1992, Annals of the CIRP, 41/1, 117.

Shimada, S., Ikawa, N., Tanaka, H., Ohmori, G., Uchikoshi, J., and Yoshinaga, H., 1993, Annals of the CIRP, 42/1, 91.

Shimada, S., Ikawa, N., Tanaka, H., and Uchikoshi, J., 1994, Annals of the CIRP, 43/1, 51.

Shimada, S., 1995, Int. J of Japan Soc. Prec. Eng., 29, No.4, 283.

Stower, I. F., Belak, J. F., Lucca, D. A., Komanduri, R., Rhorer, R. L., Moriwaki, T., Okuda, K., Ikawa, N., Shimada, S., Tanaka, H., Dow, T. A., Drescher, J. D., Proceedings of the ASPE Annual Conference, 100.

Taniguchi, N., 1983, Annals of CIRP, 32, 2.

Vitek, V., 1996, MRS Bulletin, 2, 20.

APPENDIX 1

STEPS INVOLVED IN CONVENTIONAL MD SIMULATION OF NANOMETRIC CUTTING

MD simulation of nanometric cutting involves setting up of the workmaterial and tool (either FCC or BCC), estimation of potential energy and kinetic energy of the system, moving the tool in the direction of cut and tracking the trajectory of the atoms. This demands a sophisticated computer program that can perform the above stated functions in minimal runtime. This section provides a brief explanation of the program used for conventional MD simulation and consequently on which modifications were made to implement LRMD simulation technique.

The computational parameters and the general information required for the simulation are read from a data file by the program. The general information includes the run number (to differentiate individual simulations), bulk temperature, reset constant, and time step for integration. The computational parameters are the cutting speed, depth of cut, rake angle, clearance angle, tool rotation angle, dimensions of the tool and the workmaterial, lattice constants, type of lattice structure, boundary conditions etc. of the tool and the workmaterial respectively, and Morse potential parameters between atoms of the tool, the workmaterial, and the interface (between the tool and the workmaterial).

The program sets up the lattice of the workmaterial and the tool based on the appropriate lattice structures, lattice constants, and dimensions read from the input data file. Then the boundary conditions are applied to the tool and the workmaterial. If the side is declared as boundary then the program lists the last layers of the side as boundary atoms which represents the bulk of the tool and the workmaterial that do not take part in the simulation. The rest of the workmaterial and tool atoms are listed as moving atoms. One layer adjacent to the boundary atoms are called peripheral atoms and are listed in a separate array. The momentum of these atoms are adjusted every one fifth of the period of vibration of the atom to simulate transfer of energy from the moving atoms of the tool and the workmaterial to the rest of the corresponding body.

For the calculation of potential energy of the tool and the workmaterial, Morse potential function is used. The parameters of Morse potential function for the tool and the workmaterial are established from the sublimation energy, the Debye temperature, and the minimum distance between two atoms in the lattice of the tool or the workmaterial respectively. Cutoff radius is the radius of a hypothetical sphere around an atom beyond which the potential energy of the bond between the atom at the center of the sphere and the atom outside the sphere is less than 4% of maximum potential between the two atoms. Only the bonds that fall inside the sphere are considered. This facilitates in the reduction of the computational time.

There are three pairs of arrays in the program that stores the pairs of atoms within the cutoff radius. These arrays store the atoms of the workmaterial, the tool, and the tool-workmaterial interface that satisfy the above stated condition. Within a pair of array, the first array stores the atom under consideration and the second array stores the atom index that forms a

bond with the atom under consideration (within cutoff radius). The potential energy of the workmaterial and tool is estimated only for the bonds whose length is less than the associated cutoff radius using the appropriate pairs of arrays. The force between two atoms forming a bond is the derivative of potential energy of the bond between the atoms considered. Therefore, the force on each atom is calculated for atoms within the cutoff radius.

Since some sides of the workmaterial and the tool lattice are free, there are no forces from these free sides and the resultant force on the atoms along the free side is not zero. There is a procedure in the program to relax all the forces and make the resultant force on all atoms as zero. When the atoms are in the relaxed position the potential energy of the lattice is at a minimum.

During the relax procedure the trajectory of the atoms is found by integrating the Newton's equations of motion using Runge-Kutta method. At each step the potential of the lattice is calculated and compared with the potential energy of the previous step. If the potential energy is less than the compared value the integration continues. On the contrary the velocities of all atoms are reset to zero and the integration of Newton's equation of motion is resumed. In the present code the number of such iterations is constrained to 20.

Associated with the room temperature, atoms have some kinetic energy. After relaxing the atoms of the tool and the workmaterial lattice, the velocity of each atom is found using Maxwell-Boltzman distribution. The tool is moved in the direction of cut by moving the boundary atoms of the tool (if the tool is deformable) or by moving all atoms of the tool (if the tool is infinitely hard) by a distance determined by cutting speed and time step (cutting speed x time step). The position and velocity of all atoms of the tool and the workmaterial at the end of the movement can be calculated by

integrating Newton's equations of motion by Runge-Kutta method. At the end of each time step the arrays used to store the pairs of atoms within cutoff radius are refreshed and the resultant force on each atom is calculated using Morse potential energy function. This procedure of moving the tool and calculating the resultant force is performed iteratively till the tool reaches the prespecified position.

The program stores the horizontal and vertical forces of cutting. It can also be used to store the atom coordinates at different points during the cutting procedure.

VITA

Nagasubramaniyan Chandrasekaran

Candidate for the Degree of

Master of Science

Thesis: LENGTH RESTRICTED MOLECULAR DYNAMICS (LRMD) SIMULATION OF NANOMETRIC CUTTING

Major Field: Mechanical Engineering

Biographical:

Personal Data: Born in Madras, India, On Feb 15, 1974, the son of V. Chandrasekaran and T. V. Vijayalakshmi.

Education: Received Bachelor of Engineering degree in Mechanical Engineering from University of Madras, India in May 1995. Completed the requirements for the Master of Science degree with a major in Mechanical Engineering at Oklahoma State University in May 1997.

Experience: Project Engineer, Jet-In-Park, India, from Jan. 1995-may 1995. Research assistant in Council for Scientific and Industrial Research, India, from Jun 1995-Nov. 1995. Teaching assistant in Oklahoma State University, from Jan. 1996-May 1996 and Research assistant in Oklahoma State University from May 1996-present.

Professional Memberships: Phi Kappa Phi, Indian Society for Technical Education